Published in "Advanced Materials doi: 10.1002/adma.201704463, 2018"
which should be cited to refer to this work.

# Nanoparticle–Cell Interaction: A Cell Mechanics Perspective

*Dedy Septiadi,* Federica Crippa, Thomas Lee Moore, Barbara Rothen-Rutishauser, and Alke Petri-Fink**

**Progress in the field of nanoparticles has enabled the rapid development of multiple products and technologies; however, some nanoparticles can pose both a threat to the environment and human health. To enable their safe implementation, a comprehensive knowledge of nanoparticles and their biological interactions is needed. In vitro and in vivo toxicity tests have been considered the gold standard to evaluate nanoparticle safety, but it is becoming necessary to understand the impact of nanosystems on cell mechanics. Here, the interaction between particles and cells, from the point of view of cell mechanics (i.e., bionanomechanics), is highlighted and put in perspective. Specifically, the ability of intracellular and extracellular nanoparticles to impair cell adhesion, cytoskeletal organization, stiffness, and migration are discussed. Furthermore, the development of cutting-edge, nanotechnology-driven tools based on the use of particles allowing the determination of cell mechanics is emphasized. These include traction force microscopy, colloidal probe atomic force microscopy, optical tweezers, magnetic manipulation, and particle tracking microrheology.**



## 1. Introduction

Nanoparticles (NPs) have emerged in recent decades as exciting materials for biomedical applications (e.g., drug delivery, imaging contrast, theranostic medicine, and biosensing), and in parallel the study of fundamental bio–nano interactions has grown.[1–3] For the most part, researchers have focused on the effect of specific physicochemical properties on NP cellular uptake, cytotoxicity, and in vivo biokinetics, systemic toxicity and NP fate.[4–8] However, fewer studies have focused on studying the effect of particles on cell mechanics, i.e., study on force–cell structure relationship and how it relates to cellular functions.[9] Cell mechanics are critical indicators for cell functionality and health, and these processes drive important biological activities such as cell migration, differentiation, wound healing, and tissue integrity (i.e., adhesion of cells to the extracellular matrix (ECM) and even the ECM production). Thus, it is worthwhile to investigate how NPs may affect cell mechanics and influence specific cellular functions, physiological conditions, or development of diseases.

The field of cell mechanics has been heavily studied and is well-described.[10] In general, the fundamental understanding of cell and tissue mechanics are constructed by two major cellular constituents, namely cellular adhesion system and the cytoskeleton. The cellular adhesion system comprises different structures (e.g., cell–cell and cell–ECM junctions) and proteins (e.g., integrins, cadherins, and selectins), and enables the cells to probe external force from their environment (both the ECM and neighboring cells). This system mechanically connects the cell surface, the cytoskeleton, and the cell's external surrounding. It has been long understood that cells can "feel" their external environment, and thus mechanical inputs to a cell can modulate the most basic cellular processes, such as cell migration, cell division, and differentiation.[11–14] On the other hand, the cytoskeleton exerts force on its surrounding to reshape the ECM via dynamic assembly and disassembly of cytoskeleton proteins (e.g., actin and tubulin) and motor protein complexes. The cytoskeleton is also involved in cell migration, for example, during wound healing and cancer metastasis, and in part regulates cell elastic properties, as broadly investigated by cell mechanics measurements.[15–19]

As particles can interact with cellular organelles and cytoskeletal structures, it is intuitive to imagine that particles (i.e., nano and micrometer size) can affect or inhibit their associated cellular functions, or be used to probe the environments in which cells interact. Moreover, the improvement of nanofabrication techniques has resulted in increasing application of micro- and nanoparticles towards probing cellular mechanics. Here, we aim to explore from two different perspectives this emerging field of bionanomechanics, the study of biomechanics using nanoscience tools. Specifically, we explore (i) how nanoparticles influence cell mechanics, and (ii) how nanoscience tools can incorporate particles to investigate cell mechanics (**Figure 1**).

Inherently, bionanomechanics is an interdisciplinary field built on the expertise of biologists, toxicologists, physicists, bioengineers, materials scientists, and chemists. Thus, we aim to emphasize the interdisciplinary nature involved in this research and facilitate communication between fields. First, we survey

Dr. D. Septiadi, F. Crippa, Dr. T. L. Moore, Prof. B. Rothen-Rutishauser, Prof. A. Petri-Fink
Adolphe Merkle Institute
University of Fribourg
Chemin des Verdiers 4, 1700 Fribourg, Switzerland
E-mail: dedy.septiadi@unifr.ch; alke.fink@unifr.ch
Prof. A. Petri-Fink
Department of Chemistry
University of Fribourg
Chemin du Musée 9, 1700 Fribourg, Switzerland

the effect of NPs on cell adhesion and cytoskeleton organization, which influences cell stiffness and migration dynamics. Second, we elaborate on the application of particulate materials (i.e., microparticles and NPs) to study the mechanical property of the cells—this includes the use of engineered particles as extracellular and intracellular probes to study force exerted by the cells on their environment, and the corresponding mechanotransduction pathways as well as rheological properties of the cell.

This *Progress Report* is intended and written for broad scientific community with the aim to provide a global understanding of particle–cell interactions in the context of cell mechanics. Future direction in bionanomechanics research is expected to lead to a new standardized protocol especially for scientists and industries in addressing the influence of NPs on human and animal's toxicity from point of view of cell mechanics.



## 2. Effects of Intracellular Nanoparticles on Adhesion, Cytoskeleton Organization, Cell Stiffness, and Cell Migration

### 2.1. Introduction to Cell Mechanics

Cell mechanics is a subfield of biophysics that focuses on mechanical properties of cells and their relationship with certain biological behaviors.[20] It has been long understood that cell mechanics play an important role, not only in basic cellular functions such as cell proliferation, differentiation, apoptosis, polarization, adhesion, and migration, but also in more complex activities including embryonic development, cancer metastasis, as well as wound healing. Moreover, it has been reported that the progression and development of certain diseases (e.g., atherosclerosis, heart failure, asthma, pulmonary fibrosis, preeclampsia) is directly associated to cell and tissue mechanics (also reviewed in ref. [21]), highlighting the importance of cell mechanics in development, physiology, and diseases.

Tissue/organ development is perhaps considered as the "oldest" field describing cell mechanics. The concepts of cell mechanics are generally related to two distinct processes: force generation by the cell body and force transmission through adhesive complexes.[22] Changes in the size and shape of the cell during development (e.g., motility and reorganization), for example, depends on mechanical activities of cytoskeleton, an interconnected intracellular network of filamentous polymers and regulatory proteins.[10] In addition, cells interact mechanically with their surrounding (i.e., extracellular matrix and neighboring cells) through cell–cell and cell–matrix adhesions. These adhesions, which involve many different proteins and their complexes, together with the cytoskeleton components provide important mechanical functions: (i) allowing the cell to exert mechanical forces on its environment, and (ii) detecting mechanical stimulation from the environment and transducing these mechanical signals (mechanotransduction) into a biological response (or responding through cytoskeletal reorganization and force generation). Cellular adhesions and cytoskeletons have been shown to drive development and tissue self-assembly. In particular, adhesion has been shown to drive

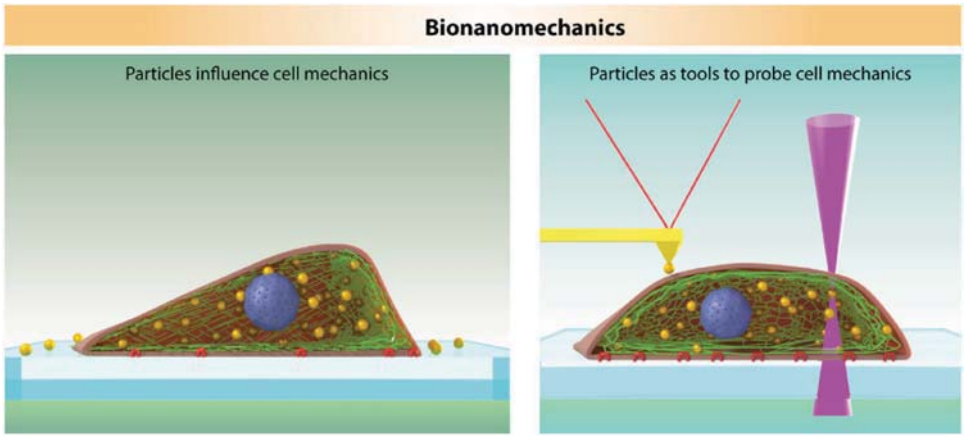


**Figure 1.** Bionanomechanics encompasses two different topics: (i) the influence of NP on cell mechanics (i.e., cell adhesion, cytoskeleton, cell stiffness, and migratory property of the cells) and (ii) the application of particles to probe cell mechanics, including rheological properties and mechanotransduction pathways.



cellular sorting (i.e., the rearrangement of scattered mixtures of two or more cell types into homogeneous clusters[23]) during tissue assembly to specific locations based on the type and density of adhesion proteins.[24]

It has been shown that environmental effects, genetic mutations, pathogens, or perturbations to the mechanical properties can disrupt the cytoskeletal architecture of the cells and further lead to the alteration of cell mechanics.[20] For instance, it was demonstrated that adhesion behavior,[25] cytoskeleton organization (including cell polarization and elongation)[26] and traction forces[27] from different types of cells varied when the cells were grown on substrates with different stiffness. Micro-[28] and nanotopography[29] have also been described to induce changes in cell adhesion, cytoskeletal organization, and the mechanical properties in human cells.

Due to their nanosize combined with unique physicochemical properties, internalized NPs are expected to interact with the cell membrane,[30] cytoskeletal structures,[31] and organelles[32] and as a consequence alter specific cellular functions. Contrary to the extensive number of cell viability studies, the impact of NPs on cell mechanics has been less thoroughly investigated. Therefore, an understanding of any possible alteration of cell mechanics following NP exposure is needed to enhance our comprehension of nanomaterial–cell interactions. This particular chapter focuses on the impact of NPs in cell–cell and cell–matrix adhesion, cytoskeletal building blocks (actin/tubulin/intermediate filament system), cell stiffness and cell migration. Substrate environment parameters, which have been shown to influence cell mechanics,[33,34] are not considered in the discussion of Section 2, since for most in vitro experiments the cells were cultured in similar conditions (i.e., on commercial glass cover slips), hence the cell mechanics responses which are described are only associated to the NP–cell interaction.

### 2.2. Influence of NPs on Cellular Adhesions

When the cells contact a substrate (i.e., the ECM, other cells, or tissues), the first cellular response will be adhesion or adherence. In a biophysical term, adhesion can be described as the bonding of two distinct entities (e.g., cell to cell/tissue, or cell to the ECM) in a manner that resists their subsequent separation, normally through either homotypic or heterotypic protein-protein interactions.[23] Transmembrane adhesion proteins (also called cell adhesion molecules or CAMs) such as immunoglobulin superfamily CAMs (IgSF CAMs), selectins, integrins, and cadherins have important functions in adhesion. In particular integrins form connections between cells and the ECM, while cadherins connect cells with other cells/tissues. The ECM itself is mainly composed of a variety of versatile polysaccharides (such as proteoglycan) and fibrous proteins (e.g., collagens, elastin, fibronectin, and laminin) which are secreted locally by the cells and assemble into an organized meshwork whose purpose is mainly to provide support for the surrounding cells (i.e., to hold cells and tissues together) and an organized lattice through which cells migrate and interact with each other.[35] Depending on their functional classification, cell adhesions or junctions can be classified into three classes. First, occluding junctions (also called tight junctions) which form an impermeable barrier across the epithelial cell layer, second, communicating junctions (or gap junctions) which allow the transport of small molecules between the cells, and third, anchoring junctions which connect the cytoskeleton of the cell (e.g., F-actins and intermediate filaments) to its neighbors or to the ECM.[35] Anchoring junction includes focal adhesion (FA) for cell–ECM adhesion, hemidesmosomes for cell-basal lamina adhesion, adherens junctions and desmosomes for cell–cell adhesion (**Figure 2**). Cell adhesion plays an important role in homeostasis and regulation of cell biological behavior including cell communication (reviewed in ref. [36]).

The presence of cell-associated NPs (either internalized or strongly attached to the cell membrane) has been shown to alter many cellular processes, e.g., provoking cell death. In particular, the examples discussed below reveal that NPs could indeed induce damage to cell adhesions. It is important to underline that there is no clear proof or explanation regarding the mechanism by which NPs might interact with cell adhesion proteins or alter adhesion-related signaling pathways. Mostly these conclusions are based on experimental observations,

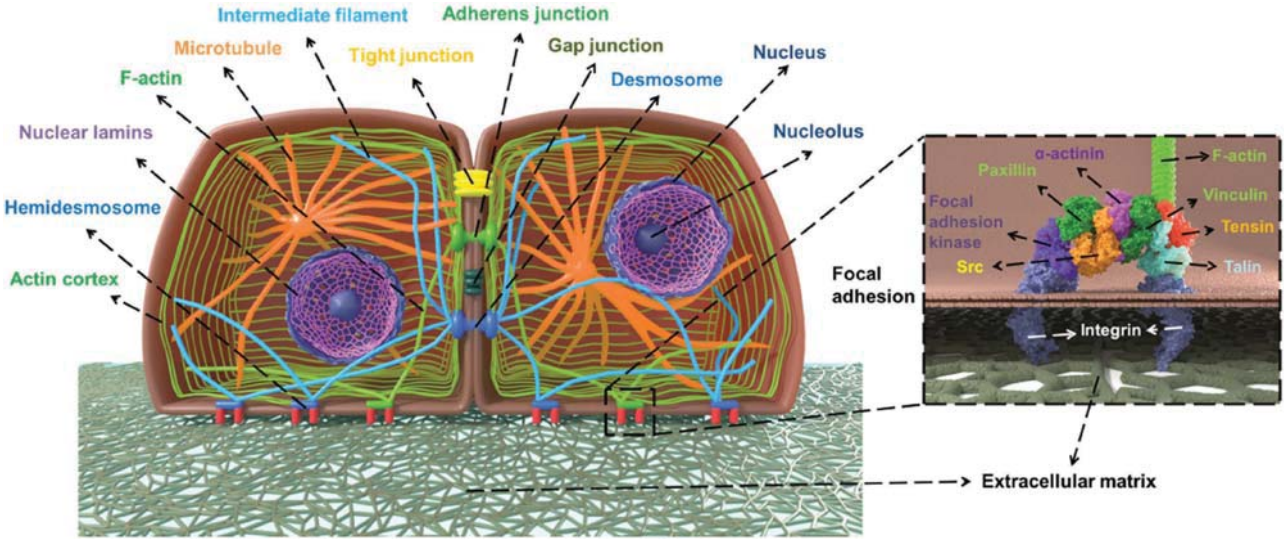


**Figure 2.** Left: Schematic representation of the cell cytoskeleton (i.e., F-actins, microtubules, and intermediate filaments), structures, and cell adhesion junctions and molecules (i.e., gap junction, adherens junction, tight junction, desmosome, hemidesmosome, and focal adhesion). Right: Different FA adaptor proteins.

hence the observed impact can be understood as a result of a complex, unknown processes. To the best of our knowledge, only limited investigations have been performed and mostly focused on cell–ECM adhesion, adherence, and tight junction.

The disruption of tight junction by NPs was observed by Xu et al.[37] Using a coculture blood brain barrier (BBB) model of rat brain consisting of microvascular endothelial cells, pericytes, and astrocytes, they were able to demonstrate that silver NPs (AgNPs) could induce destruction of the tight junctions and allow the particles to trancytosis through the BBB. They showed that after 24 h treatment, AgNPs at initial concentration 10 μg $mL^{-1}$ significantly decreased transendothelial electrical resistance (TEER) values compared to a control "no particle" sample (TEER for control experiments and with AgNPs were ≈200 and 160 Ω $cm^2$, respectively). Further analysis using immunostaining and fluorescence microscopy revealed the reduction of tight junction protein expression, namely zonula occludens-1 (ZO-1), as characterized by the absence of continuous, smooth, pericellular, belt-like structures which were detected in the control cells. They also observed severe mitochondrial shrinkage, vacuolations, and endoplasmic reticulum expansion in the astrocytes.

Setyawati et al.[38] performed investigations into detrimental impact of NPs on adherens junctions, demonstrating that titania ($TiO_2$) NPs caused endothelial cell leakiness by disturbing the hemophilic interaction of adherens junction protein, VE-cadherin. They observed that NP treatment on human lung microvascular endothelial cells (HMVEC) resulted in tyrosine phosphorylation of VE-cadherin at intracellular residues (i.e., Y658 and Y731), loss of interaction between VE-cadherin and p120 as well as β-catenin, and degradation of VE–cadherin (**Figure 3**a). Similarly, Long et al.[39] showed that a negatively charged mercaptoundeonic acid-capped AgNPs affected retinal vascular permeability through activation of the plasma contact system, and disruption of the adherens junctions. In vitro experiment using human retina endothelial cells (HREC) revealed that these NPs activated the plasma kallikrein–kinin system (KKS) by triggering Hageman factor autoactivation. The activation of KKS led to the release of bradykinin, which further activated B2 receptors and induced the shedding of VE-cadherin.

IgSF CAM family proteins, such as vascular cell adhesion molecule VCAM-1,[40] intercellular adhesion molecule ICAM-1,[41] or selectin family member, endothelial cell leukocyte adhesion molecule ELAM-1[42] are some adhesion molecules which mediate endothelial adhesiveness in endothelial cells. Increasing endothelial adhesiveness itself is commonly associated to an increase of endothelial cell dysfunction, which is frequently observed in the development of cardiovascular diseases such as atherosclerosis.[43] Previous studies have shown higher induction (expression) of these molecules in alumina NP-treated porcine arterial endothelial cells (PEC) and human umbilical vein endothelial cells (HUVEC), resulting in the increase of the cell adhesiveness. Increased adhesiveness was further shown to instigate the recruitment of monocytes on the endothelial layer, indicative of an inflammatory response initiation.[44]

The effect of intracellular NPs on cell–ECM adhesion can be monitored from the formation of FAs, clusters of integrin receptors which are formed through the binding of the transmembrane protein integrin and integrin binding motifs on the ECM. FAs are mechanically linked to F-actin cytoskeleton (see dedicated section for actin cytoskeleton in Section 2.3). The presence of FAs in the cells can be directly visualized by staining cytoskeletal FA adaptor proteins, e.g., vinculin, talin, paxillin, α-actinin, to name some (Figure 2). To understand the dynamics of cellular adhesion upon NP interaction, FA parameters such as FA number and FA size/area (for studying FA maturation) warrant consideration. De Cuyper and co-workers[45] observed a linear decrease of vinculin FA area and number, as well as an increase in cell polarization upon increasing the concentration of intracellular superparamagnetic iron oxide NPs (SPIONs) in human blood outgrowth endothelial cells (HBOEC). In the presence of NPs, the FA area was reduced by

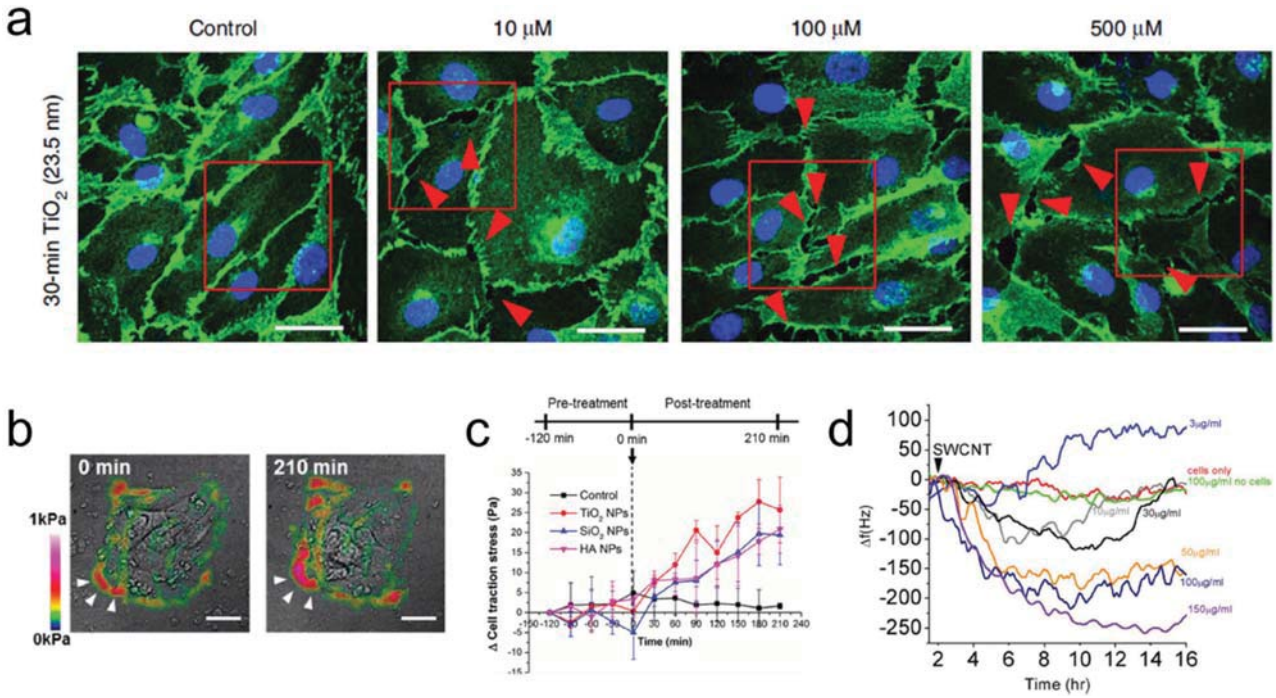


**Figure 3.** NPs induce damage in cell adhesions. a) Confocal microscopy image of the VE-cadherin of HMVECs (green). Leaking between the cells (red arrow) was observed in the $TiO_2$ NP-treated sample in contrast to the control cells which showed no leaks. Reproduced with permission.[38] Copyright 2013, Springer Nature. b) Traction force map of TR146 epithelial cells post $SiO_2$ NPs exposure and c) real-time cell traction stress profile as a function of time and type of NP treatments. Adapted with permission.[49] Copyright 2014, American Chemical Society. d) Time-dependent response of adherence of macrophages on gold-coated QCM surface in the presence of different concentrations of SWCNTs. Reproduced with permission.[57] Copyright 2011, Springer.

half with respect to nontreated cell samples. Small FA size was attributed to newly formed adhesion points due to high levels of actin cytoskeleton remodeling. In addition, a significant reduction of focal adhesion kinase (FAK) expression, a cytoplasmic tyrosine kinase that plays a critical role in integrin-mediated signal transductions,[46] was also observed.[45] Similarly, using quantitative fluorescence imaging, Hou et al.[47] reported the amount of vinculin in mesenchymal stem cells (MSC) was lower after incubation with $TiO_2$ NPs, which is in agreement results previously reported by Wu et al.,[48] who showed the disappearance of vinculin spots in HUVEC and a decrease in FAK expression after treatment with SPIONs. Moreover, Leong and co-workers[49] observed higher occurrences of long vinculin near the vicinity of the cell–cell boundary (Figure 3b), indicating that oral mucosa cells (TR146) are highly contractile upon treatment with silica ($SiO_2$), $TiO_2$, and hydroxyapatite (HA) NPs.

The physicochemical properties of particles might be expected to dictate particular cell mechanics response(s). However, to the best of our knowledge, there are no systematic reports accounting for the influence of NPs properties apart from size/dimension and dose on cell mechanics. Thus, it will be critical to introduce these parameters in the future bionanomechanics research. Previously, the reduction of cell adhesion after exposure to $TiO_2$ particles was reported in 2010 by Saldaña and Vilaboa.[50] They demonstrated the reduction of FA area and colocalization of paxillin FAs with phospho-focal adhesion kinase p-FAK (Tyr-397), which further led to a decrease in cell adhesive strength (i.e., a very rapid detachment of $TiO_2$-treated human osteoblastic Saos-2 cells during cell detachment assays). However, in their in vitro experiment, only micrometer-size particles were used. In addition, Hou et al.[47] observed size-dependent effects on adhesion dynamics, where less vinculin FAs were detected after MSC were treated with large (108 nm) $TiO_2$ particles compared to smaller NPs (14 nm). In the other direction, Pöttler et al. showed the dose-dependent adhesion after NP treatment. Cell adhesion was determined by counting the number of attached cells. Cells treated with SPIONs up to 20 μg $cm^{-2}$ showed no significant alteration of adhesion for rabbit vocal fold fibroblasts (VFF). However, exposure of 40 and 80 μg $cm^{-2}$ SPIONs resulted in a significant decrease in VFF adhesion.[51]

As briefly mentioned, exact mechanisms of how NPs alter the adhesion property of cells are still debatable. Mokhtari et al.[52] reported the significant inhibitory effects of SPIONs-polyethylene glycol (PEG)-cisplatin on the adhesion of the human mammary gland T47D cells may be due to the inhibition of $\alpha 2\beta 1$ integrin mRNA expression. Vieira et al.[53] and Pan et al.[54] showed a reduction of ECM-associated protein production (i.e., collagen and laminin) due to the presence of AgNPs, gold nanoparticles (AuNPs), and $TiO_2$ NPs. Collagen itself is an abundant ECM protein which provides binding site for FAs. Disruption of the expression of collagen might have direct influence on the structural integrity and function of actin stress fibers (nonmuscle cell contractile actin bundles) since these fibers are generally anchored to integrins which bind to secreted ECM proteins. Another possible explanation is the induction of cell death by NPs, since it is well known that dying cell lose their adherence.

Traction force microscopy (TFM) can be used to determine the strength of cell–ECM adhesion (or cell traction force/stress, CTF; see dedicated TFM part in section 3.1.2). In the absence of NPs, human dermal fibroblasts (HDF) exerted robust traction forces along their periphery (CTF > 500 Pa), indicating stronger adhesion. However, $TiO_2$ NPs exposure resulted in reduced cell area with weaker traction force (CTF < 300 Pa).[54] This finding however, was not supported by results published later by Leong and co-workers.[49] They observed relatively strong traction force applied by TR146 epithelial cells in the presence of $SiO_2$, $TiO_2$, and HA NPs (CTF > 100 Pa) in comparison to the control sample (CTF < 75 Pa). Furthermore, they simultaneously observed maturation of FAs and the promotion of an adhesive cell phenotype (Figure 3c,d).[49] Different values of the traction force observed for those two cases can be attributed to the difference in cell type. For example, it has been shown that metastatic cells such as MDAMB231 human breast adenocarcinoma, PC3 human prostatic cell carcinoma, and A549 human lung epithelial carcinoma possess higher traction stress compared to their nonmetastatic counterparts, e.g., MCF10A human breast epithelial cell line, PrEC human primary prostate epithelial cells, and BEAS-2B human bronchial epithelial cells (CTF > 400 Pa vs CTF < 120 Pa).[55]

Distraction of cellular adhesion upon NPs treatment can be monitored using quartz crystal microbalance (QCM) measurements. QCM is a very sensitive nanogram mass sensing device and has been widely used to monitor and quantify adsorption and deposition of materials on the surface of a piezoelectric crystal. Any change of the crystal's oscillation frequency due to dynamic processes occurring on the surface, including cellular adhesion and readhesion, can be detected. In the presence of human hepatoma HepG2 cells, Wei et al.[56] observed a quite large shift of QCM frequency (≈700 Hz) due to a strong adhesion between the cells and the QCM surface, as well as the changes in mass and viscoelasticity of cells on the gold substrate at 0–4 h. Within the next phase (4–18 h), a slight decrease in frequency shift of the crystal indicated cell detachment, spreading and re-(adhesion). Introduction of AuNPs or a mixture of AuNPs and paclitaxel, a microtubule stabilizing drug, to the cells resulted in the decrease of the frequency shift (to ≈150 or 500 Hz for AuNPs and AuNPs and paclitaxel, respectively). This indicated more cell detachment. Wang et al.[57] similarly used QCM to study the adhesion properties and cytotoxic response of DH82 macrophages upon incubation with single-walled carbon nanotubes (SWCNTs). Without SWCNTs, no change in oscillation frequency was detected while for SWCNTs-treated macrophages a significant frequency decrease was observed (Figure 3e). They suggested that the difference of adhesion and migration properties of nonphagocytotic mode (in the absence of nanotubes) and phagocytotic macrophages (in the presence of SWCNTs) could be responsible for the frequency change.

### 2.3. Effects of NPs on Cellular Cytoskeletal Structures

The cytoskeleton has several basic functions: (1) to organize the contents of the cell, (2) to physically and biochemically connect the cell to the environment, (3) to generate forces enabling the cell to move and change shape, and (4) to provide contractility and help in cell division.[10,35,58] In eukaryotic cells, the cytoskeleton is made of three filamentous proteins, namely actin microfilaments (filamentous actins or F-actins), microtubules (MT) and intermediate filaments (IF). F-actins are formed through polymerization of actin monomers (also called globular actin or G-actin), while MT are constructed from polymerization of alpha and beta tubulin, in which the nucleation of the polymerization is mediated by gamma tubulin.[35] IF on the other hand are composed of different proteins that are expressed in variety types of cells, including keratins, vimentin, neurofilament proteins, nuclear lamins, and nestin.[59] In particular, nuclear lamins are important for the structural properties of the nucleus (especially nuclear membrane/nuclear envelope), and the regulation of numerous nuclear processes including DNA replication, transcription and chromatin organization.[60]

In order to understand the effect of NPs on cytoskeletal integrity, we must first understand any possible physicochemical interactions between NPs and the main cytoskeletal proteins. Indirect interaction of NPs and cytoskeleton has been shown by Nienhaus and co-workers[31] where they demonstrated that NP-carrying vesicles (i.e., intracellular quantum dots trapped in endosomes/lysosomes of HeLa cells) were actively transported along MT with a speed of ≈0.4 μm $s^{-1}$, similar to the transport rate of kinesin. However, it is not known how NPs, which are normally compartmentalized inside endosomes/lysosomes rather than freely "swimming" in the cytoplasm, could affect cytoskeletal structures. The only evidence comes from fibers such as carbon nanotubes (CNTs) which, depending on their aspect ratio, can be found inside the cytoplasma[61] and could possibly directly interact with F-actin as proven by computer simulations.[62,63] Furthermore, Dawson and co-workers[64] revealed the presence of intracellular tubulin (i.e., alpha and beta tubulin) in the protein corona formed around $SiO_2$ NPs, and this finding has brought a growing interest in the domain of NP-protein interaction. For example, by using different techniques such as dynamic light scattering, UV–vis spectroscopy, circular dichroism (CD) spectroscopy, hyperspectral imaging, and transmission electron microscopy (TEM), Wen et al.[65] probed the interaction between cytoskeletal proteins and citrate-coated 30 nm AgNPs. Most likely, the NPs interact with these structural proteins through electrostatic, van der Waals, and hydrophobic interactions or hydrogen bonding. They also observed an increase in hydrodynamics size and zeta potential, a red-shift of the plasmonic band of AgNPs upon binding, as well as changes to the secondary structures of actin and tubulin which might affect their polymerization properties (**Figure 4**a,b). Similarly, Choudhury et al.[66] investigated the binding and aggregation properties of tubulin heterodimers and the inhibition of MT polymerization in the presence of AuNPs in cell-free systems using UV–vis, CD, Raman and Fourier transform-infrared spectroscopies.

The interaction of actin/tubulin with NPs observed in vitro was found to have a rather negative impact on cytoskeletal integrity. Although the numbers of studies is limited, the majority of findings showed destabilization and degradation of actin filaments in cell samples containing NPs. Pernodet et al.[67] demonstrated that "bioinert" AuNPs induced aberrant F-actin formation. In vitro experiments using HDF showed the formation of actin "dots" rather than long stress fibers, a

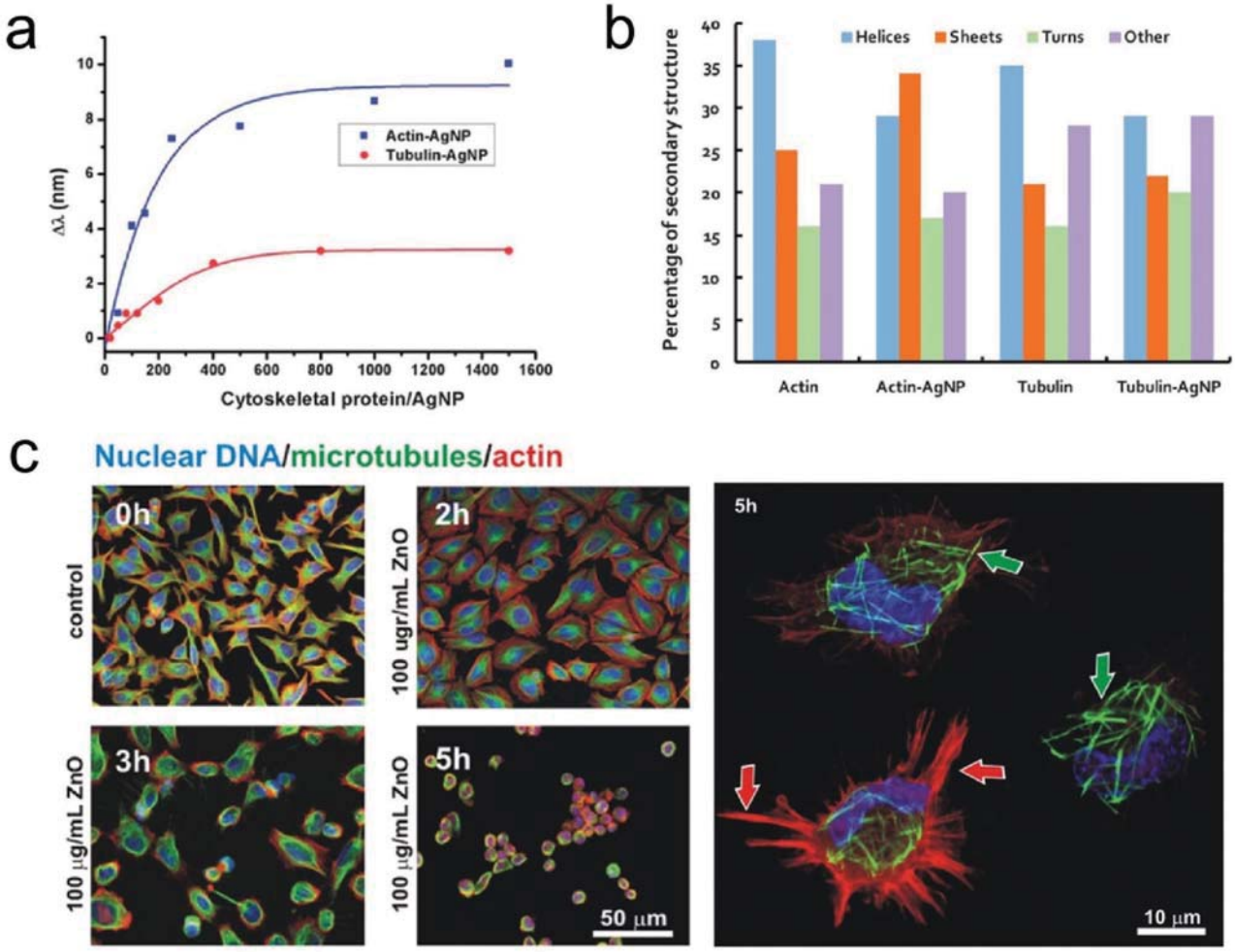


**Figure 4.** Probing the interaction between NPs and cytoskeletal proteins. a) The red shift of AgNPs' plasmonic band was induced by the formation of two main cytoskeletal protein–AgNP corona. Plasmonic peak of naked AgNPs is 406 nm. b) Alteration in the secondary structures of actin and tubulin upon their binding with AgNPs. Adapted with permission.[65] Copyright 2013, The Royal Society of Chemistry. c) Confocal microscopy image showing aberrations in the organization of the actin microfilaments (red channel) and microtubules (green channel), including F-actin spikes (red arrows) and MT straightening, thickening, and shortening (green arrows) post zinc oxide (ZnO) NP treatment. Reproduced with permission.[69] Copyright 2016, The Royal Society of Chemistry.

reduction of F-actin fiber size and density, as well as a decrease in cell area by nearly a factor of two at all concentrations of AuNPs used (up to 800 μg $mL^{-1}$). Next, Vieira et al.[53] reported an alteration in cytoskeletal organization, including a change of cell polarity and the increase of F-actin fiber formation, in HDF treated with AuNPs and AgNPs. Another result suggested that exposure of zinc oxide (ZnO) NPs to RAW 264.7 mouse macrophages resulted in F-actin depolymerization and a decrease in the level of F-actins.[68] Fanarraga and co-workers[69] observed a reorganization of actin microfilaments into cell bundles and formation of aberrant F-actin trails affecting proliferation and viability of human keratinocytes (HaCat) and cervical cancer cells (HeLa) after ZnO NPs treatment (Figure 4c). It was speculated that the dissolution of ZnO in the lysosome to $Zn^{2+}$ allowed the binding of $Zn^{2+}$ to the actin network caused this perturbation, since it is known that actin contain $Zn^{2+}$ binding sites and this binding could disturb the self-assembly of actin microfilaments.[69] Moreover, exposure of HBOEC to SPIONs has caused significant F-actin remodeling, thus leading to a decrease in cell area and polarization.[45] This study is in agreement with previous reports by Wu et al.[48] and Gupta et al.[70] in HUVEC and human fibroblast following treatment with SPIONs and gelatin NPs, respectively. Decrease or loss of F-actins itself could lead to destabilization of the cytoskeleton, cell architecture and furthermore induce permanent injury to the cells or even cell death.[71]

Apart from detrimental effects on the F-actin microfilament networks, NPs have been similarly shown to influence MT network polymerization and further induce MT destabilization and dysfunction. For example, disorganized structures (including straightening, thickening, and shortening of MT) were observed in ZnO NP-treated HaCat and HeLa cells,[69] and SPION-exposed endothelial cells.[45] A similar result was found by Leong and co-workers,[49] whereby internalization of $SiO_2$, $TiO_2$, and HA NPs by TR146 cells was shown to lower the level of MT acetylation, destabilize the MT networks and further affect the homeostatic regulation of intracellular tension. These impacts included the loss of intracellular

filamentous MT, an increase in F-actin remodeling, and the maturation (elongation) of vinculin FAs. Previously, it has been demonstrated that cell exposure to $TiO_2$ particles led to a disorderly arrangement of $\beta$-tubulin and acetylated $\alpha$-tubulin fibers, reduction in the number of actin ventral stress fibers and a reduction in overall cell adhesion area.[50] Additionally, NPs induced damage to the MT network not only through inhibition of MT polymerization, but also through aggregation of tubulin heterodimers. Fluorescence microscopy data of NP-treated A549 and MCF-7 human breast cells showed that AuNP treatment destroyed MT, disrupted cell morphology, and shrank the cellular periphery while the control cells displayed normal structure.[66] Through in situ MT de-polymerization/re-polymerization experiments and quantification of fluorescence intensity of stained MTs in A549 cells, Gonzalez et al.[72] have demonstrated the decrease in MT acetylation following treatment with $SiO_2$ NPs. In agreement with previous result,[49] they demonstrated that MT were less acetylated after NPs treatment, thereby indicating a lower level of MT stability. The change of the MT network in the presence of NPs, however, does not always correspond to lower levels of microtubule acetylation. Apopa et al.[73] reported increased levels of MT acetylation in human microvascular endothelial cells (HMEC) due to the induction of reactive oxygen species following exposure to SPIONs.

In neuronal cells, microtubule-associated proteins, namely tau proteins, play a major role in MT polymerization and axon growth.[74] In vitro interaction between tau proteins and NPs such as iron NPs[75] and CNTs[76] have been previously described in the literature. Based on a recent study in SH-SY5Y neuroblastoma cells by Mao et al.,[77] the interaction between $TiO_2$ NPs and tau proteins resulted in a decrease in MT density, disorganization, and disruption of MT. Furthermore, treatment of primary rat cortical neurons (PRCN) with AgNPs resulted in the loss of cytoskeleton components such as $\beta$-tubulins and F-actins, as well as the reduction of a number of synaptic clusters of the presynaptic vesicle protein synaptophysin, and the postsynaptic receptor density protein PSD-95. Exposure to AgNPs caused a reduction in $\beta$-tubulin branching and overlapping, a decrease in the degree and intensity of fluorescent phalloidin (a tool in the study of actin networks at high resolution), and finally cell death.[78]

### 2.4. Effect of NP Uptake on Cell Stiffness

Cell stiffness (or the opposite of cell elasticity) can be defined in simple terms as the resistance of the cell to an externally induced deformation. It is commonly expressed by the Young's modulus ($E$), the ratio between the stress (force sustained by the sample over its cross section area) and the applied strain (with unit in Pascals).[79] Increase or decrease in cell stiffness is often associated with a change in cell physiology and leading to a diseased state. Previous findings have revealed the role of the cytoskeleton in conferring stiffness and contractility to the cells,[80] as well as the relationship between the cytoskeleton/cell stiffness in context of tumors/cancer malignancy. Malignant tumor cells for example, are found to be softer than benign and healthy ones (reviewed in ref. [9]). In healthy cells with a relatively high degree of stiffness, actin microfilaments are generally well organized, resulting in a larger Young's modulus. In cancerous cells these organized structures are not apparent or less observed, hence the cells are softer and more flexible.[18,79] Usually, cell stiffness is measured through indentation experiments using atomic force microscopy (AFM; see dedicated part of AFM in Section 3.2.1).[81] Earlier we have described the detrimental effects of NPs on the F-actin microstructure, and as expected, the stiffness of the cells will be reduced by NPs. Pi et al.[82] demonstrated that intracellular selenium (Se) NPs could induce membrane bio-mechanical property changes in MCF-7 cells by disturbing actin microfilaments and the transmembrane adhesion protein CD44. AFM experiment clearly indicated that control MCF-7 cells had a much higher Young's modulus than SeNPs-treated MCF-7 cells (5.05 ± 2.43 MPa vs 0.69 ± 0.31 MPa), indicating that MCF-7 cells were much softer after Se NPs treatment (see **Figure 5**a).

The following studies, however, suggest the opposite effect. Thus, NP-induced changes to cell stiffness actually involve mechanisms that are more complex. Ogneva et al.[83] reported an increase in cell stiffness of about 2.5 times for $SiO_2$ NP-treated MSC compared to control cells (≈1 pN/nm for control cell and 2.66 pN $nm^{-1}$ for $SiO_2$ NP-treated MSC). They claimed the changes might arise due to alterations in protein content (i.e., F-actin/G-actin ratio), followed by the reorganization of the cortical cytoskeleton and modification of

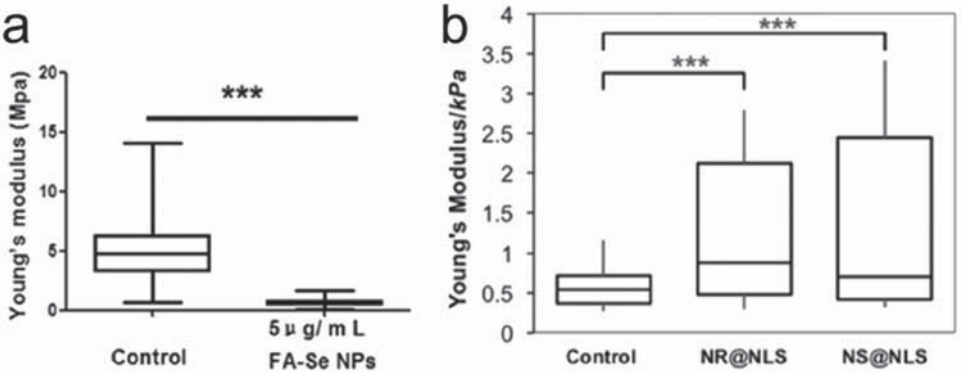


**Figure 5.** NPs impair cell stiffness. a) Comparison of Young's modulus ($E$) values between control and SeNPs-treated MCF-7 cells. Reproduced with permission.[82] Copyright 2013, Elsevier. b) Stiffness plots from single cells post nuclear-targeted AuNP and AuNR treatment. Reproduced with permission.[85] Copyright 2017, American Chemical Society.

cell surface. A transient increase of G-actin in the cytoplasm was attributed to the dissociation of F-actin to G-actin, which in turn initiated different signaling pathways. Using single cell compression-based AFM, Zimmer et al.[84] determined the cellular stiffening of human aortic endothelial cells (HAEC) in the presence of ZnO NPs. The parameter for cell stiffening was expressed as relative deformation ($\varepsilon$) which is defined as the change in height of the cell over the initial height or relative volume deformation (RVD), which is denoted as displaced volume over the initial cell volume. The lower the $\varepsilon$ or RVD value, the higher the observed stiffness. They found out that at a low ZnO NP dose (i.e., 10 μg $mL^{-1}$), cells were stiffer in comparison to untreated cells. Increasing the concentration to 50 μg $mL^{-1}$, however, led to significant changes in cell morphology (i.e., cell swelling) and surprisingly a right-shifted RVD value indicating softening. They suggested that the higher uptake of ZnO by membrane and intracellular components would lead to heterogeneity of the cell membrane, ion flux dysfunction (swelling), as well a weakening of the cytoskeleton. As opposed to ZnO, $SiO_2$ NPs did not induce any similar response even after the concentration was increased (50 μg $mL^{-1}$) and no detectable changes for both height and volume of the cells were observed upon NP treatment. These data however, contradict the previous conclusion by Ogneva et al.[83] Another related example was shown very recently by El-Sayed and co-workers.[85] They reported that nuclear membrane targeted AuNPs enhanced cell nucleus stiffness when introduced to HEY A8 ovarian cancer cells (Figure 5b). The localization of AuNPs and gold nanorods (AuNRs) in the nuclear membrane of the cells, due to targeting of the nuclear localization signal (NLS), led to the increased expression of IF inner nuclear membrane lamin A/C protein, and further added mechanical stiffness to the cell nucleus. Berntsen et al.[86] also measured changes to the stiffness and contractility of human airway smooth muscle cells (HASMC) after different NP exposure using a different technique, namely optical magnetic twisting cytometry. They concluded that cell contractility was decreased by ZnO (40–100 nm) and copper(II) oxide (CuO; 50 nm) NPs treatment, while $TiO_2$ NPs (25 nm) caused no effect.

### 2.5. Effect of NPs in Cell Motility

Cell migration/locomotion/movement/motility plays an important role in tissue formation during embryogenesis, wound healing or immune response such as white blood cells movement to inflammation/injury sites. Impaired cell migration during all stages of development lead to severe embryonic malformations ranging from early embryonic lethality to birth defects and multiple human syndromes (e.g., neurological disorders, congenital heart diseases, and physical and mental retardation).[87] In order to migrate, there are four major steps cells have to perform: (1) polarization of cell body (establishment of a front-to-rear polarity axis/leading-to-trailing edge), (2) protrusion/extension of cellular membranes or lamellipodia, thin, sheet-like membrane protrusions located at the leading edge, (3) formation of new adhesions on the underlying ECM, and (4) translocation/cell body retraction. It has been shown that NPs are able to inhibit or alter the speed of the cell locomotion through different mechanisms. Previously, we have briefly mentioned that the cytoskeleton, mainly F-actins and MT, provides important roles and functions in cell motility; hence, any modification in cytoskeletal structure and function will affect the migration properties of the cells. Gonzalez et al.[72] demonstrated that a decrease in MT acetylation reduced the speed of A549 cell movement following $SiO_2$ NP treatment. Disruption of F-actin and MT further retarded cell migration in cells following incubation with SPIONs[48] or ZnO NPs.[68]

A second pathway by which NPs inhibit cell migration is associated with cell adhesion. Strong traction forces and maturation of FAs will not only promote stable anchorage of the cells on the substrate, but also lead to a retardation of cell migration. Leong and co-workers[49] reported that $SiO_2$, $TiO_2$ and HA NPs treatment of TR146 cells promoted the destabilization of MT networks and the formation of mature vinculin FAs, increased cell traction and retarded collective cell migration. By using a scratch-based wound healing assay, they showed that NP-treated cells reduced cell migration in a dose-dependent manner by 60–70% with respect to nontreated cells (**Figure 6**a,b). Interestingly, cells pre-treated with monodansylcadaverine, a substance used to block the uptake of NPs, almost completely restored their migration ability indicating that the internalized NPs significantly retard cell migration.[49] However, it is worth mentioning that with low adhesion, cells will not be able to exert enough force to pull the cells forward during the body retraction step.[88] The latter has been shown by Hou et al.,[47] where treatment of MSC cells with $TiO_2$ significantly decreased the adhesion of the cells (i.e., reduced vinculin FAs) and reduced cell migration. By using a matrigel invasion assay, they observed that the cells

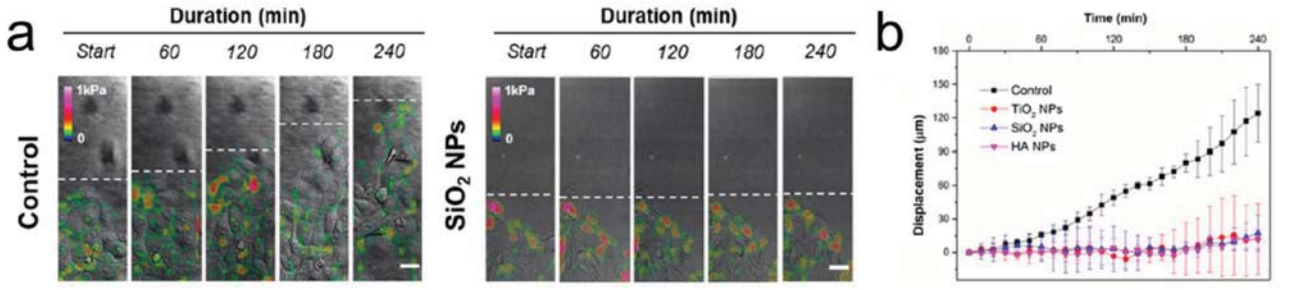


**Figure 6.** NP influence on cell migration. a) Brightfield images show retardation of cell sheet migration of TR146 epithelial cells in the presence of $SiO_2$ NPs. b) Displacement profile of the cells in the presence of three different types of NPs. Reproduced with permission.[49] Copyright 2014, American Chemical Society.

treated with 14 nm NPs had a higher relative migration in comparison with 108 nm $TiO_2$ NP-treated cells.

The final mechanism by which NPs can inhibit cell migration is by altering the expression of cell migration-related proteins/molecules. Vieira et al.,[53] reported the reduction of human fibroblast migration speed after AuNP and AgNP treatment, even at low concentration (1–10 μg $mL^{-1}$): both particles decreased the deposition of ECM by fibroblasts (i.e., a decrease in collagen and laminin deposition was observed), change the expression of ECM receptors in particular integrin-type receptors (very late antigen 2, $\alpha 2\beta 1$ integrin (VLA-2) and very late antigen 6, $\alpha 6\beta 1$ integrin (VLA-6)), and alter the cytoskeletal organization. AgNPs have been also shown to downregulate the expression of epidermal growth factor receptor (EGFR). Overexpression of EGFR is often associated to cancer prognosis and metastasis, and has been shown to enhance cell migration in human breast cancer cells and NIH3T3 fibroblasts.[89] Analysis of EGFR expression in AgNP-treated A549 cells after overstimulation with external EGF showed a significant decrease of EGFR mRNA expression, resulting in the retardation of cellular migration in a wound healing assay.[90] NPs were also able to upregulate expression of microRNA miR-34a which has itself been shown to target and downregulate Ras-related C3 botulinum toxin substrate 1 (Rac1) protein,[91] a protein involved in actin polymerization and cytoskeletal organization, including the formation of lamellipodia.[92] Bhattacharya et al.[93] have shown the thymoquinone-encapsulated PEG NPs could significantly increase the expression of miR-34a through tumor protein p53, and further down-regulated Rac1 expression followed by actin depolymerization. They observed a significant reduction in lamellipodia or filopodia (i.e., thin, spiky actin-rich plasma-membrane protrusions) formation on the surface of human breast cancer cell line MCF-7 and HBL-100, thus retarding cell motility. This finding however, did not support the previous results by Kang and co-workers[94] where they reported that ZnO NPs caused activation of Rac1 and cell division control protein 42 homolog (Cdc42), the latter related to formation of filopodia in HUVEC.[95] Production of adenosine triphosphate (ATP) in the mitochondria was also influenced by the presence of intracellular NPs. A recent report has described a mechanism whereby bovine serum albumin-coated AuNRs inhibited mitochondrial oxidative phosphorylation and glycolysis, which resulted in a major reduction of ATP production and subsequently inhibited F-actin assembly. Formation of lamellipodia in AuNRs-treated NIH-3T3 fibroblast, B16F10 melanoma, and PC3 prostate cancer cells was repressed, and cell migration and invasion ability was reduced. Similar behavior was confirmed in vivo in a nude mouse model.[96] Expression of putative ATP-dependent RNA helicase DEAH (Asp-Glu-Ala-His) box helicase 15 (or DHX15) in human gastric cancer cell lines (MKN28 and BGC823) has been found to increase after the cells were treated with cerium oxide NPs.[97] The increased expression of DHX15 could activate p38 mitogen-activated protein kinases (MAPK) signaling pathway,[98] further leading to an inhibition of proliferation and metastasis of the cells.[99] Abrogation of MAPK signaling pathway in AuNP-treated A2780 human ovarian carcinoma cells was already observed previously by Mukherjee and co-workers,[100] and a reduced activation of vascular endothelial growth factor receptor 2 (VEGFR2) which regulates endothelial migration and proliferation[101] was also reported. Du and co-workers[102] proposed that AuNPs were able to bind VEGF165 protein and indirectly reduce VEGFR-2 activation in HUVEC. Using a Transwell wound healing assay, they showed that cells which were treated with VEGF165 in the presence or absence of AuNPs possessed different migration properties: inhibition in cell migration in NPs-treated cells was monitored.

Contrary to many reported studies regarding cell motility retardation, Liu et al.[103] observed an increase in A549 and 95D lung cancer cell migration activity after treatment with less than 10 nm size citrate-capped AuNPs. This may be associated with the increased expression of two key modulators of cell invasion, namely matrix metalloproteinase 9 and ICAM-1. High expression of both proteins generally is connected to advanced stages of cancer. Separately, increased motility speed of Schwann cells (SC), a glial cell in the peripheral nervous system in the presence of SPIONs was reported by Huang et al.,[104] however it was only possible when alternating magnetic field was turned on. They observed an enhanced migration along the direction of magnetic field. SPIONs stimulated SC to cross the astrocytes-SC boundary via integrin-mediated mechanotransduction.

### 2.6. Lessons Learned from NPs and Cellular Mechanics

The number of in vitro and in vivo toxicity studies of NPs has risen dramatically over the years; however, the availability of information regarding alteration of cell mechanics due to interaction with NPs is still limited. Nonetheless, recent findings have shown that NPs can modulate the mechanical behavior of cells. The influence of different parameters including particle type, physicochemical properties and cell culture conditions influencing cell mechanics in vitro is summarized in **Table 1**. The similarity we could observe is the fact that most of the administered NPs were mostly particles without any surface functionalization, and it is well-known that many of these nonfunctionalized particles have been shown to induce toxic effects in different cell types.[105–108] In addition, we noticed that there is still not any systematic study regarding this topic. Moreover, most of our current knowledge comes from nanotoxicity studies where researchers are investigating potentially adverse effects of NPs on cells/organisms. Therefore, there is potential for bias to view NPs as harmful, but in reality there is a necessity to perform more research about possible effects of NPs on cell mechanics at subtoxic concentrations. In fact, the exact mechanisms of toxicity for each NP type are still incomplete,[105] and perhaps bionanomechanics could provide a mechanistic understanding of this phenomenon. Even though it is too early to predict, we are convinced that in the future the effect of NPs in the context of cell mechanics can be combined with classical viability study to better understand and asses the hazard and safety of nanomaterials.

The field of bionanomechanics is in its nascent phases, therefore plenty of investigations and studies are possible. From the materials chemistry point of view, the influence of, e.g., surface functionalization, size, shape, concentration, etc. on cell mechanics still needs to be thoroughly investigated. From a biological point of view, the cell type needs to be considered, especially to address whether effects on cell mechanics are cell-dependent or not. Information on any possible effects

**Table 1.** Cell mechanics responses depending on particle type.

| Particle type | Size, zeta potential, and surface functionalization | Administered dose and incubation time | Cell types used | Impacts on cell mechanics | Ref. |
|---|---|---|---|---|---|
| AgNPs | 101 ± 12 nm; −7.9 ± 0.6 mV | 1 and 10 μg mL$^{-1}$; 24 h | BBB consists of microvascular endothelial cells, pericytes, and astrocytes | Increase in BBB permeability and expression of tight junction protein ZO-1 | [37] |
| | 9.7 ± 0.9 nm; −38.3 ± 0.8 mV; mercaptoundeonic acid | 0.2 and 2 μg mL$^{-1}$; 5–60 min | HREC | Destruction of adherence junctions (VE-cadherin) through activation of the plasma KKS | [39] |
| | 10 nm; citrate | 0.1–10 μg mL$^{-1}$; 24 h | Human skin fibroblast CCD1072Sk | Reduce in ECM production and cell migration, change in cell polarity and the increase of F-actin fiber formation | [53] |
| | 20 nm | 1–50 μg mL$^{-1}$; 3 d | PRCN | Destruction of $\beta$-tubulins and F-actins | [78] |
| | 100–150 nm | 1–50 μg mL$^{-1}$; 48 h | A549 | Retardation of cellular migration through decrease of EGFR mRNA expression | [90] |
| Alumina | 10–20 nm (single) and ≈500 nm in culture media (CM) (aggregates) | 1.0–250 μg mL$^{-1}$; 40 h | PEC and HUVEC | Increase of the protein expression VCAM-1, ICAM-1, and ELAM-1 indicating increase in cell adhesiveness | [44] |
| AuNPs | 10 nm | 0.1–10 μg mL$^{-1}$; 24 h | Human skin fibroblast CCD1072Sk | Reduce in ECM production and cell migration, change in cell polarity and increase in F-actin fiber formation | [53] |
| | 13 ± 1 nm; citrate | 0–800 μg mL$^{-1}$; 6 d | HDF | Formation of actin "dots" rather than long stress fibers, a reduction of F-actin fiber size and density, as well as a decrease in cell area | [67] |
| | 20–60 nm | (0.5–25) × 10$^{-12}$ M; 12–72 h | A549 and MCF-7 | Inhibition of tubulin polymerization | [66] |
| | ≈35 nm (for spherical NPs) and 25 × 6 nm (for rod); 14.9 ± 3.13 mV (for rod shape) and 18.3 ± 7.55 mV (for spherical NPs); nuclear localization signal | Up to 5 × 10$^{-9}$ M; 24 h | HEY A8 | Enhancement of cell nucleus stiffness through increase expression of IF inner nuclear membrane lamin A/C protein | [85] |
| | ≈15 nm | 125 × 10$^{-9}$ and 250 × 10$^{-9}$ M; 24 h | HUVEC | Reduced activation of VEGFR-2 which regulates endothelial migration | [102] |
| | 5 and 10 nm; citrate | 50 μg mL$^{-1}$; 48 h | A549 and 95D | Increase in lung cancer cell migration activity through increased expression of matrix metalloproteinase 9 and ICAM-1 | [103] |
| AuNRs | ≈54 × 18 nm; FBS protein | (25–200) × 10$^{-6}$ M; 24 h | MDA-MB-231, PC3 and B16F10 | Inhibition of F-actin assembly through reduction of ATP (energy) production and retardation of cell migration | [96] |
| Cerium oxide | ≈3 nm; −18 mV | 0.01–10 μg mL$^{-1}$; 3 d | MKN28 and BGC823 | Increase expression of DHX15 which further lead to inhibition of metastatic activity of the cell | [97] |
| CuO | 40–100 nm | Up to 15 μg mL$^{-1}$; 16–22 h | HASMC | Decrease in cell contractility | [86] |
| Gelatin | 37 ± 0.84 nm | 0.2 mg mL$^{-1}$; 4 h | Infinity™ telomerase-immortalized primary human fibroblasts (hTERT-BJ1 | Disruption of F-actin and MT structures | [70] |
| HA | 49 ± 14 nm (single), 236 ± 9 nm (aggregates); −6.5 ± 0.2; | 125 × 10$^{-6}$ and 1250 × 10$^{-6}$ M; 12 h | TR146 | Increase of long vinculin near the cell–cell boundary and traction force, maturation of FAs, low level of MT acetylation, destabilization of MT networks, promotion of an adhesive cell phenotype and retardation in cell migration | [49] |
| Se | 40–90 nm; −40 mV | 2.5 and 5 μg mL$^{-1}$; 6 h | MCF-7 | Destruction of F-actins and reduce of membrane stiffness | [82] |
| $SiO_2$ | 15 ± 3 nm (single), 236 ± 25 nm (aggregates); −13.1 ± 1 mV | 125 × 10$^{-6}$ and 1250 × 10$^{-6}$ M; 12 h | TR146 | Increase of long vinculin near the cell–cell boundary and traction force, maturation of FAs, low level of MT acetylation, destabilization of MT networks, promotion of an adhesive cell phenotype and retardation in cell migration | [49] |

**Table 1.** Continued.

| Particle type | Size, zeta potential, and surface functionalization | Administered dose and incubation time | Cell types used | Impacts on cell mechanics | Ref. |
|---|---|---|---|---|---|
| | 59–174 nm; –7.74 to –17 mV | 7.5–211 μg mL$^{-1}$; up to 40 h | A549 | Decrease in MT acetylation and migration velocity | [72] |
| | 7 nm | 50–100 μg mL$^{-1}$; 1–24 h | MSC | Increase in cell stiffness ≈2.5-fold than control cell | [83] |
| SPIONs | 132.4 nm; –25.37 mV; | 20, 40, and 80 μg cm$^{-2}$; 24 h | VFF | At higher concentration (e.g., 40 and 80 μg cm$^{-2}$ SPIONs) resulted in a significant decrease in VFF adhesion | [51] |
| | 4–14 nm; –31.3 ± 7.3 mV; lipids, dextran, carboxydextran and citrate | 500–1000 μg mL$^{-1}$; 4 and 24 h | HBOEC | Decrease of vinculin FA area and number as well as increase in cell polarization, reduction of focal adhesion kinase (FAK) and F-actin remodeling | [45] |
| | <10 nm | 12.5–100 μg mL$^{-1}$; 5 h | HMEC | Increase in MT acetylation and endothelial cell permeability | [73] |
| $TiO_2$ | 23.5 nm (single) and 57.1 nm (aggregates) | $10 \times 10^{-6}$ M; 30 min | HMVEC | Endothelial cell leakiness through degradation of VE–cadherin | [38] |
| | 14, 108, and 196 nm | 50, 100, and 200 μg mL$^{-1}$; 3, 7, and 14 d | MSC | Reduce of expression of vinculin FA adaptor and cell migration | [47] |
| | 21 ± 8 nm (single), 272 ± 4 nm (aggregates); –7.1 ± 1 mV | $125 \times 10^{-6}$ and $1250 \times 10^{-6}$ M; 12 h | TR146 | Increase of long vinculin near the cell–cell boundary and traction force, maturation of FAs, low level of MT acetylation, destabilization of MT networks, promotion of an adhesive cell phenotype and retardation in cell migration | [49] |
| | 3.32 ± 2.39 μm | 0.5–2.5 mg mL$^{-1}$; 1–24 h | Human osteoblastic Saos-2 cells | Reduction of paxillin FA area and decrease in cell adhesive strength, disorderly arrangement of $\beta$-tubulin and acetylated $\alpha$-tubulin fibers, reduction in the number of actin ventral stress fibers and in overall cell adhesion area | [50] |
| | 15.0 ± 3.5 nm (single NP) and 200 ± 13 nm (aggregates) | 0.4 and 0.8 μg mL$^{-1}$; 30 min to 2 d | HDF | Decreases in cell area, traction force, cell proliferation, mobility, and ability to contract collagen | [54] |
| | 20.90 ± 3.57 nm (single) and 110.0 ± 72.9 nm (aggregates in CM); –0.73 ± 1.27 mV in CM and –142.56 ± 19.80 mV in water | 0.1–100 μg mL$^{-1}$; 24 h | SH-SY5Y | Disorder, disruption, retraction, and decreased intensity of MT | [77] |
| ZnO | 200–250 nm; –0.56 mV | Up to 500 μg mL$^{-1}$; 24 h | Mouse macrophage RAW 264.7 | Depolymerization and degradation of F-actin and inhibition of cellular migration | [68] |
| | 86 ± 3 nm | 15–100 μg mL$^{-1}$; 24–96 h | HaCat and HeLa | Reorganization of actin microfilaments into cell bundles, formation of aberrant F-actin trails and rigid macrotubes (i.e., straightening, thickening and shortening) of MT | [69] |
| | 100–200 × 20–70 nm | 10 and 50 μg mL$^{-1}$; 4 h | HAEC | Increase of cell stiffness at low dose (e.g., 10 μg mL$^{-1}$) and decrease of cell stiffness at higher dose (50 μg mL$^{-1}$) | [84] |
| | 40–100 nm | Up to 15 μg mL$^{-1}$ | HASMC | Decrease in cell contractility | [86] |
| | 93.35 ± 14.53 nm (single) and 126.2 ± 120.4 nm (aggregates) | 0.1–100 μg mL$^{-1}$; 24 h | HUVEC | Activation of Rac1 and Cdc42 protein which induce formation lamellipodia and filopodia | [94] |

on cell-basal lamina adhesion (i.e., hemidesmosomes, FAs) and cell–cell adhesion (i.e., desmosomes, adherens junctions) are needed to draw a general idea of the impact of NPs on cell adhesion. The study of NP interactions with IF and cytoskeletal mechanosignaling pathways needs to be addressed. In addition, theoretical studies using suitable biophysical models for recapitulating NPs and cell mechanics should be performed.

A general conclusion of this previous chapter is presented as follows:

*Take-Home Messages:*

- Cell mechanics plays important role in organism development, physiology and diseases.
- Ag,[37,39] alumina,[44] HA,[49] SPIONs,[45,51] $SiO_2$,[49] and $TiO_2$ NPs[38,47,49] can induce detrimental effects on cell adhesion including destruction of tight and adherens junctions and modulation of cell–ECM adhesion (i.e., reduction and maturation of FAs).

- Interaction of Ag,[37,53] HA,[49] SPIONs,[45] $TiO_2$,[49] and ZnO[68,69] NPs and cytoskeletal proteins (actin and tubulin) can promote destabilization of the cytoskeleton including remodeling and destruction of MT and F-actins structures.
- Cell stiffness increases due to the presence of Au[85] and $SiO_2$ NPs.[83]
- NPs can retard cell migration through destruction of the cytoskeleton,[68,72] increase in adhesions[49] and modulating the expression of cell migration-related proteins/molecules.[53,90,93,96,102]

## 3. Particles as a Tool to Study Cells Mechanics

Because the study of how particle properties can have an impact on cell mechanics is an emerging field, there is a need for tools to investigate cell mechanics behavior. To this point, rapid progress in the field of particle-based technologies has enabled the utilization of particles as tools to study a myriad of cellular phenomena: Particles, because they can directly interact with subcellular structures, are ideal candidates to study cell mechanics. Fluorescent, metallic/plasmonic or magnetic micro- and NPs are widely used materials for sensing, and current efforts have been dedicated to implementing particles in cells as in vitro probes. Particle technologies have enabled researchers to develop new methods and probe cellular phenomena/mechanical properties (e.g., cell forces exerted on the ECM, cell stiffness and cytoplasmic viscosity, strength of cellular interactions, and translation of mechanical forces into biochemical signals). To be certain, studying the influence of particles on cell mechanics is tied to the utilization of particles to study these very same processes. For example, particle-based techniques offer a valid method to directly investigate how internalized NPs alter cell stiffness and modify cellular forces. Thus, we describe here the (emerging) methods by which particles can act as tools to study cellular mechanics and cell mechanical properties.

### 3.1. Micro and NPs to Study the Interaction between Cells and the ECM

Nanotechnology-driven tools including microscopy and (micro and nano)particles-based characterization techniques have been widely used to probe cell–substrate/ECM interaction, i.e., the effect of the substrate on cellular behavior and the force that the cells exert on the substrate (traction force). Synthetic surfaces/substrates are used to mimic the ECM, thus allowing concomitant study of the interaction of the cells with their external environment and how this affects cell physiology and behaviors. The forces generated by the cells during adhesion, spreading and migration can be quantified, for example, by using TFM, a technique that strongly relies on the displacement of micro and nanotrackers embedded in elastic substrates. To ease the understanding in TFM, we wish first to provide information regarding the use of NPs in and as cell substrates.

#### *3.1.1. NPs in Cell Substrates*

In tissues, cells attach to the ECM through cell–ECM adhesion. Apart from its biochemical and structural properties, physical features of ECM such as its rigidity, density, porosity, insolubility and topography (i.e., spatial arrangement and orientation)[109] are very important aspects which dictate cell–ECM response.

In fact, it is well-known that the nanotopography of a surface can play a significant role in cell development, cell mechanics and migration.[29,110] It is therefore intuitive that nanoscale objects can be regarded as an alternative platform to mimic the ECM structures. Furthermore, by incorporating NPs onto a surface, it is possible to control and engineer specific surface geometry/physical characteristics. To this point, ECM-like surfaces can be fabricated by creating synthetic substrates with defined patterns of specifically functionalized NPs. Thus, beyond exploiting the possible benefits of nano and micro particle-decorated surfaces, these particles can be used as a tool to understand the mechanism behind cell adhesion and spreading,[111–119] migration[120,121] and differentiation.[122–125]

In order to realize particle-based substrates as a surface for studying cell mechanics, particles must frequently be functionalized to provide selective adhesion. ECM ligands (arginine-glycine-aspartic acid (RGD)-based motifs) linked to the NPs surface are often used to promote cell adherence.[114–116,120,122,126] However, a single binding motif alone is not guaranteed to promote cell–substrate interaction, FA assembly, and spreading. Rather, this action is mediated by ligand interaction, particle spacing and ligand density. Schenk et al.[117] developed a substrate functionalized with both cyclic RGD (cRGD)-coated AuNPs and Pro-His-Ser-Arg-Asn (PHSRN) peptides (interspaced on the substrate via a PEG molecule) which synergistically enhanced cell spreading. In vitro experiment using rat embryonic fibroblasts showed differences in the adhesion behavior on substrates functionalized with only PHSRN, cRGD-coated AuNPs, or both ligands. In particular, the two ligands alone did not promote cells-substrate interaction while their combination boosted cells attachment, FA assembly, and spreading.[117] Another basic aspect that regulates the interaction between the cells and the external environment is the spacing and density of the surface ligand. To obtain stable FAs, the distance between the integrins and ECM ligands must be close enough. This distance varies among different cell lines: for example by using functionalized AuNPs as the ECM-like substrates for rat embryonic fibroblast cells, this distance was shown to be ≤58 nm,[114] while for human breast epithelial metastatic cancer cells the distance between cRGDfk-functionalized AuNPs was relatively large (≈1.7 μm).[115]

Apart from a specific surface functionalization, particle density is also essential. Recently Li et al.[118] investigated the effect of substrates' particle density and their composition on neuron adhesion and neuritogenesis. They observed an increase in viability and neurite development for PRCN upon an increase in the concentration of amine-functionalized AuNPs (from 1 to 490 particles $\mu m^{-2}$; **Figure 7**a). Rigidity of the substrate on which particles are patterned on has been similarly shown to affect cell adhesion. Advanced work by

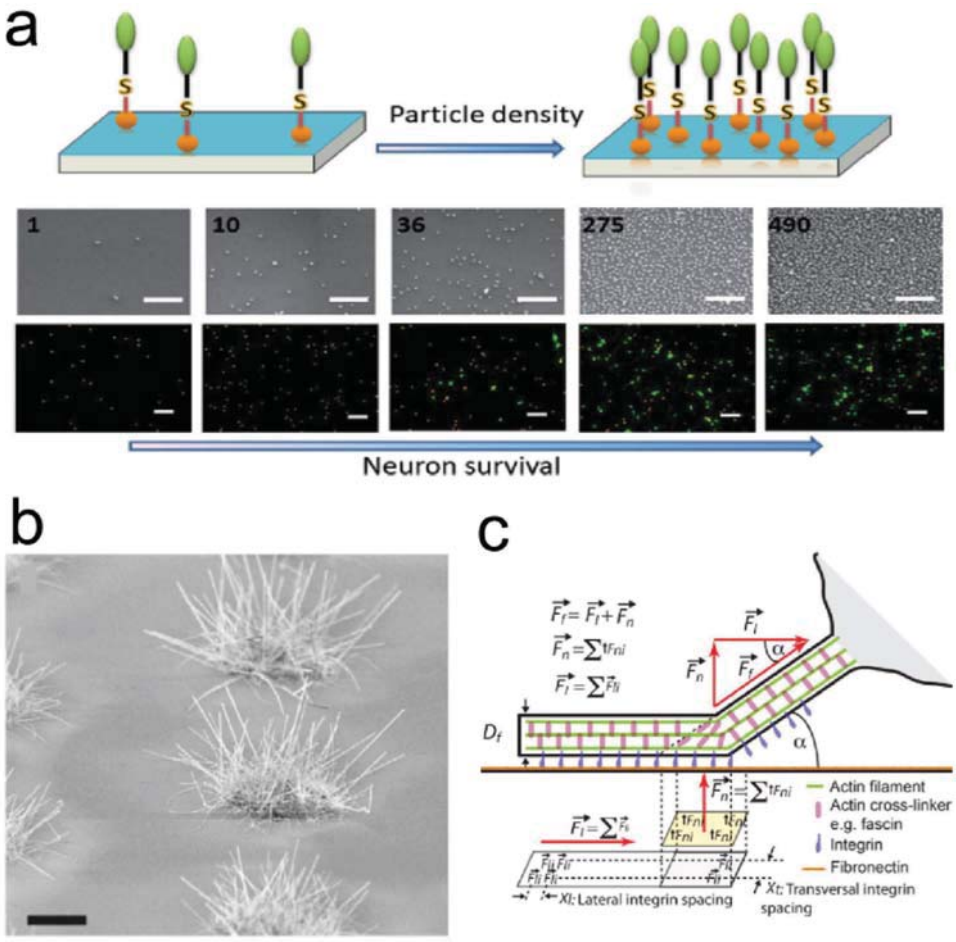


**Figure 7.** NPs mimicking the ECM are used as cell culture substrates. a) A scheme of the surface functionalization with AuNPs; scanning electron microscopy (SEM) images of surface functionalization at different coating densities and live-and-dead fluorescent staining image of neurons seeded on the surfaces. Reproduced with permission.[118] Copyright 2015, The Royal Society of Chemistry. b) SEM image of islands patterned with silicon nanowires. Scale bar 5 µm. c) The molecular zipping model schematic of the force distributions on integrins as a function of adhesion angle (α). Adapted with permission.[116] Copyright 2013, Springer.

Platzman et al.[126] demonstrated that cells which were cultured on two substrates having different stiffnesses, but similar surface functionalization, possessed different mechanical behaviors. In this work, 8 nm cRGD coated AuNPs were patterned on PEG-passivated glasses and soft PEG-diacrylate hydrogels. The patterns were hexagonal and the lateral distance between the particles was varied between 62 and 161 nm. They observed that ligand spacing and stiffness of the substrate influenced the adhesion of rat embryonic fibroblast cells, in particular the cells only attached on the substrate with a spacing of 62 nm for both glass and hydrogel substrates, while for higher spacing distances they could adhere and spread only on the hydrogel. They hypothesized that the observation came from the ability to deform the hydrogel substrate and reduce the distance between particles.

Another important aspect for cell adhesion is the interaction between filopodia and ECM-induced nanotopography, as recently addressed by Albuschies and Vogel.[116] In their work, nanoengineered substrates were used to understand how the filopodia interact with nanometric structures. Flexible hairy silicon nanowires were grown from gold seeds on a micropatterned glass surface (Figure 7b). The wires and the flat surface were both functionalized with fibronectin to avoid results biased by different ligand densities. By analyzing the adhesion dynamic of primary normal human dermal foreskin fibroblast, they concluded that filopodia steered adhesion, spreading, and division of the cells depending on the dynamics of the contact angle formed between filopodia and the substrate. On the semiflexible nanowires the filopodia aligned and adhered strongly while on the rigid flat glass, they were more prone to peel off. In the latter case, only the small portion of filopodia that created a low angle with the surface could be stabilized. A new biophysical model called the molecular zipping model was proposed to explain how filopodia adapt to the topography (Figure 7c): the filopodia probe the surface by applying traction forces on the FA, and the contact angle between the filopodium and the substrate determines whether there is adhesion or if the filopodium peels off. In particular they calculated a maximum contact angle in order to still have a strong adhesion (<12°); at higher contact angles

the traction forces cannot be sustained by the FAs and the contact is lost.

Particles can therefore be used to mimic the micro/nano-architecture and mechanical properties of ECM, or probe specific cellular behaviors. However these passive substrates fail in a sense that the ECM is a dynamic material, continually remodeling under different physiological or pathological conditions.[127,128] To overcome this limitation, different approaches have been developed including the use of stimuli-responsive polymers as cell culture substrates. To be more specific, varieties of substrates have been fabricated which are able to alter their conformation and trigger dynamic changes in the substrate stiffness and topography due to changes in temperature,[129–131] light,[132] or pH.[133] Magnetoresponsive systems such as magnetic NPs are also used in nanocomposite cell culture substrates. Mechanical stimulation of magnetic-based substrates has been achieved by applying a static and pulsatile magnetic field on magnetic substrates.[134–136] Kiang et al.[134] embedded anisotropic nickel microwires in a soft acrylamide gel substrate. They reported that microwires that were aligned in the direction of the magnetic field could be used to tune the surface roughness. In vitro experiment using A7R5 rat smooth muscle cells revealed that the cells changed their actin cytoskeletal organization by adapting their adhesion area and shape in response to a single change of topography while no significant remodeling was observed upon prolonged dynamic stimulation. Another example was shown by Mayer et al.[136] where they synthesized a magneto-active elastomer that changed stiffness and topography after application of static and oscillating magnetic field, respectively. Human fibroblasts seeded onto these substrates spread upon stiffness increase and migrated due to the pulsatile surface translocation obtained with an oscillating magnetic field. However, the employment of polydimethylsiloxane (PDMS)-based matrix did not allow a reversible stimulation of the cells since PDMS, affected by plastic deformations upon magnetic excitation, could not recover its initial shape.

Substrates decorated with NPs have therefore been broadly investigated, however their potential to study FA kinetics, mainly in dynamic conditions, have not been completely exploited. For example, responsive polymeric substrates decorated with functionalized NPs could be useful tool to study cells adhesion and spreading.

#### *3.1.2. Traction Force Microscopy*

When cells interact with the ECM/substrates, they will exert force, namely cellular traction forces (CTF), onto the substrate. This particular force originates from the actomyosin (a complex of actin and myosin motor protein) contraction and from actin polymerization. CTF are known to control cell shape, migration and other important cellular functions.[137,138] CTF are mainly observed as vectors sitting in the plane on which cells are adhering, but out-of-plane forces have been measured as well and they can be caused by cortical tension, nuclear compression, and FA rotation.

TFM is a technique that allows the determination of the CTF field at the cell–matrix interface by analyzing the substrate displacement upon cellular attachment. This technique has been implemented with different systems such as thin silicone films that create wrinkles when interacting with cells,[139] micropillar systems that bend when pulled,[140] and fluorescent particles embedded in the substrate that changed their position when the substrate surface is "stressed."[141–144] In the context presented here, we will focus on particles-based TFM that mainly utilizes fluorescent polystyrene micro and nanoparticles embedded in soft transparent substrate. CTF can be estimated using a mechanical model for the substrate (i.e., the inverse linear elasticity theory[141,145] or finite element method analysis[144,146]) upon cell-induced deformation. For complete reviews on TFM please refer to refs. [147–149]. Notably, TFM can be expanded to study 3D forces generated by cells seeded on 2D surfaces[144] or embedded in 3D scaffold.[143] Recently Legant et al.[150] developed a multidimensional (2.5D) TFM to measure how cells on planar surface extend their forces in the 3D space. They observed that FAs located on protruding and retracting peripheral regions sustained shear and normal stresses originated from out-of-plane rotational moments. For mouse embryo fibroblasts, maximum shear stresses (±550 Pa) were typically higher than the normal ones (±250 Pa) (**Figure 8**a).

Even though TFM represents the gold standard to quantify CTF, some limitations of this technique have become increasingly evident. Visualization of bead displacement, on which the force reconstruction is dependent, is subjected to numerous factors such as the optical resolution, the beads distribution, and the point spread function of the bead itself. Moreover, the Poisson's ratio of the substrate material, defined as the ratio between the transverse and the axial strain, must be precisely quantified because it influences the bead displacement,[151] and therefore affects the force reconstruction. Additionally, cells must be detached from the substrate to record the reference image, thus making it difficult to perform correlative analysis between cellular structures and the force field unless cells expressing fluorescent tags are chosen.[150,152] Another bottleneck of TFM is the cumbersome data analysis. TFM is extremely sensitive to the quality of the input data (e.g., bead position). Experimental noise can generate a substantial error in the final outcome since the solution of the inverse equation needed to calculate the CTF field (originated from the inverse linear elasticity theory) is an ill-posed problem.[149]

Nonetheless, recent works have attempted to overcome the aforementioned limitations. Colin-York et al.[152] developed a method to increase the spatial resolution and TFM accuracy by using stimulated emission depletion (STED) microscopy. By combining computer simulations and experiments, they observed that STED-TFM allowed an increase in optical resolution and improved the reconstruction of the forces generated by the cells in comparison to normal confocal microscopy-based TFM (Figure 8b). Another elegant solution to increase the spatial resolution and to allow live acquisition of in and out of plane CTFs was proposed by Bergert et al.[153] Highly deformable silicone-based substrates were decorated with monocrystalline arrays of fluorescent nanodisks fabricated by electrohydrodynamic nanodrip-printing. The nanodisks with diameter and thickness ≈200 and 30 nm were made by an assembly of fluorescent quantum dots (QDs) printed in a triangular array (Figure 8c). This printing technique increased the

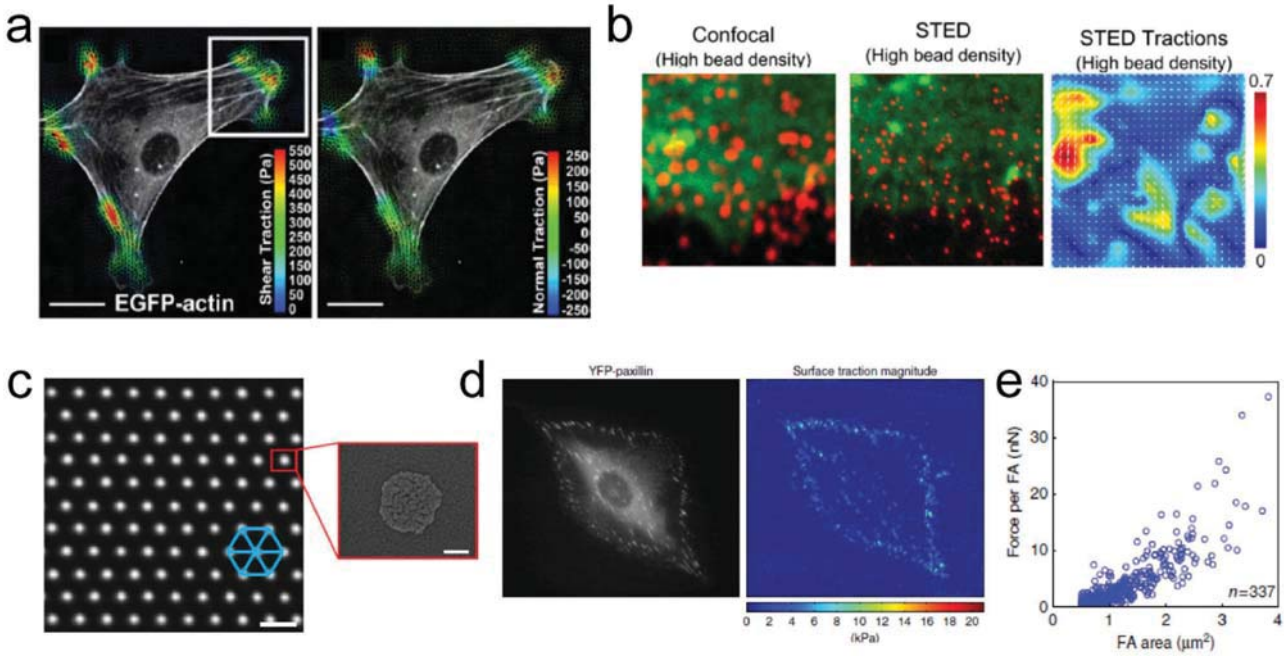


**Figure 8.** Traction force microscopy systems. a) Shear and normal traction stress vectors on the cell body. Adapted with permission.[150] Copyright 2013, National Academy of Sciences. b) Confocal and STED images of fluorescently labeled F-actins (green) and fluorescent beads (red). Traction forces fields for STED-TFM. Forces are color-coded in kPa. Adapted with permission.[152] Copyright 2016, American Chemical Society. c) Image of soft silicone substrate patterned with fluorescent nanodisks. Scale bar 2 μm. Insert: scanning electron microscopy (SEM) image of QDs in a single nanodisk. Scale bar 100 nm. d) Yellow fluorescent protein (YFP)-paxillin confocal image of embryonic fibroblasts; reconstructed surface traction forces and e) graphic depicting force per FA over FA area. Adapted with permission.[153] Copyright 2016, Springer Nature.

spatial resolution (interdisk spacing of 1.5 μm), reduced the size of the fluorescent marker (≈200 nm) and ensured a high precision in the deposition of the pattern (precision in nanodisk positioning of 30–45 nm). These substrates coated with fibronectin were tested to investigate the mechanical response of HeLa cells, embryonic fibroblasts, HUVEC, MCF10A, and PC12 cells. To calculate the displacement and the CTF field, the deformed array of nanodisks was fitted as a deformed-triangular mesh. To reconstruct the reference image, the mesh was computationally relaxed back to its original triangular configuration. It is worth noting that with this method, it was not necessary to detach the cells from the substrate and therefore a direct correlation TFM could be achieved by performing immunostaining of specific protein immediately after TFM experiments. Due to the high spatial resolution of the pattern, the forces applied by the single FA could be measured and were found in the range of 1–30 nN (Figure 8d,e). Moreover, since the nanodisks were printed on the same plane, out of plane forces could be detected; the authors observed that the cells pulled upwards at the leading edge and pushed downward toward its center. Another improvement of TFM technique has been recently achieved by Alvarez-Gonzalez et al.[151] They determined the Poisson's ratio during TFM experiment. A double layer polyacrylamide substrate was designed in which the beads are placed onto two separate planes, one near the surface and one inside the gel. By analyzing the displacement of the beads in both layers, the force field as well as Poisson's ratio could be calculated simultaneously. Finally, it is worth mentioning the work proposed by Holenstein et al.[154] in which they developed a novel CTF simulation benchmark to optimize experimental parameters and to test the accuracy of traction force reconstruction algorithms. By confirming simulation results with experiments they observed that bead distribution is critical to obtain a precise force reconstruction and that optical flow-based algorithms that track single particles displacement are more accurate than particle image velocimetry algorithms.

### 3.2. Micro and NPs as In Situ Sensors to Study Cells Mechanics

Due to size, geometry and other nano-/microspecific properties, micro- and NPs are intriguing tools to study the mechanical properties of cells compartments and to elucidate mechanotransduction pathways. Both topics are in continuous expansion and resolutive answers to some biomechanical aspects such as cellular rheology (i.e., cell stiffness and viscosity)[20] and force transduction are still unknown. In this context, micro- and NPs have been used to actively stimulate cells mechanically, or act as passive trackers to perform microrheological studies of cytoplasm. Both active and passive techniques present advantages and drawbacks. Active techniques, such as colloidal probe AFM,[17,18,67,155–163] optical tweezers,[164–167] and magnetic manipulation,[168–172] can precisely deliver controlled mechanical stimulation to specific regions of the cells, but they can be invasive and are mainly limited to cells adhering on flat substrates. Particle tracking microrheology[173–176] can be classified as a passive technique since it does not require any contact

between the cell and the external recording system and it can therefore be implemented remotely in a 3D matrix/scaffold or under flow conditions. Nevertheless, with this technique it is not possible to precisely probe specific cell organelles, rather the cell as a whole.

#### *3.2.1. Colloidal Probe Atomic Force Microscopy*

Since its invention in 1986, AFM[177] has rapidly become a prominent tool to study topography and mechanical properties of materials and surfaces.[178,179] Advanced progress in AFM technology allowing its application in liquid[180] and in controlled environments has further opened the possibility to use AFM for characterizing soft matrices such as polymeric[181] and biological systems including proteins, bacteria, and cells[157] in their pristine condition. In the context of cell mechanics, quantitative AFM has been used to analyze the mechanical (rheological) properties of a single cell and its compartments including the stiffness of the membrane as well as elasticity and viscosity of cytoskeleton and nucleus. More importantly, they have been broadly investigated in their physiological and pathological conditions.[15,16,156,159,182–186]

There are two commonly used AFM-based approaches for probing cell mechanics. One relies on the indentation of the cell membrane with a commercial nanometer-size AFM tip and the second is based on the use of spherical micron-size particles (colloidal probes) manually attached to the cantilever tip. The latter, called colloidal probe AFM, possesses several advantages over the former. First, it increases the contact area between the probe and the cell membrane, thus lowering the possibility of damaging or disturbing the cell.[155–157] Second, the large contact area averages local variations in cell rigidity, therefore less experiments are necessary to obtain reliable data.[158] Third, spherical particles help to simplify the contact geometry between the tip and the cell surface, hence simple mechanical models such as the Hertz elastic model,[178] can be applied without making severe, unrealistic assumptions on the contact area and surface forces.[158,159] However, these colloidal probes normally reduce the spatial resolution since the indentation area of microspheres can be larger than the one of a commercial conical or pyramidal tip (≈20 nm).

For the AFM tip, the choice of the microparticle in terms of size and material is fundamental to produce reliable and precise colloidal probes. The particles must be incompressible with respect to the cell membrane, must not adhere on the cell membrane and must be stable in biological media around physiological temperatures (37 °C). Hence, materials susceptible to corrosion or deformation phenomena must be avoided. To date a couple of colloidal probes have been used including polystyrene or $SiO_2$ beads, and these materials produce consistent and reliable results. In addition, due to their large contact area, colloidal probes are suitable for performing deep indentations on the cell body (≈3 μm) without perforating the cell membrane, thereby allowing the possibility to investigate the mechanical properties of subcellular structures.

Biomechanical measurements with AFM mainly rely on two types of experiments: approach and retract curves obtained by indenting the cell at constant velocity, and stress-relaxation experiments in which a specific indentation is kept constant for a defined period. To determine parameters related to the cell elasticity (i.e., Young's modulus) approach and retract curves are often fitted with Hertzian-based contact models.[17–19,160–163,187] Viscoelastic properties are obtained by fitting relaxation experiments with models derived from the Maxwell's viscoelastic theory,[156,160,187] single power-law, stretched exponential functions,[161,188,189] and modified Hertz models.[155]

Colloidal probe AFM can then be useful to retrieve the cytoskeleton mechanical properties. Indeed, the role of F-actins and myosin II motor proteins in the regulation of elastic, viscous, and long-term mechanical behavior of the cells have been broadly investigated by indentation and relaxation experiments.[15–19,163,190] Colloidal probe AFM is also a useful tool to study the mechanical properties of internal cells compartments. In 2015, Babahosseini and co-workers[156] compared the biomechanics of inner cellular regions of noninvasive or invasive cancerous breast cells, namely, MCF10A and MDA-MB-231 cells, by performing stress-relaxation tests at different indentation depths (max indentation 3 μm). The results were fitted with the Generalized Maxwell model and the cells were modeled as a triple-layered structure: plasma membrane and actin cortex (up domain), cytoplasm and nucleus (middle domain) and nuclear and integrin (low domain, **Figure 9**a). The authors showed that the lower domains are stiffer and more viscous regardless the cell type. In particular, the elastic modulus of MCF10A was reported to be ≈60, 70, and 130 kPa for the upper, middle and lower domains, respectively, while the viscosity calculated for the same cell line was 0.05, 0.3 and 6 kPa s for the upper, middle, and lower domains. They also observed that noninvasive cells were stiffer and more viscous that the malignant ones, in agreement with previously reported findings.[18,155]

The mechanical characterization of cellular compartments and the cytoskeleton based on colloidal probe AFM can be used to compare different states of the cells. Indeed this technique has been broadly used to understand the relationship between biomechanical properties and cell types,[160,187] culture media composition,[162] cell aging,[19] and carcinogenicity levels.[18,155] Iyer et al.[158] proposed an interesting study on the characterization of the surface brush layer (e.g., microvilli, microridges, and cilia, Figure 9b, top) of healthy and cancerous cervical epithelial cells. The colloidal probe itself is fundamental for this work because it increases the total contact area between the probe and this complex cell surface, thus averaging the signal and avoiding any nonlinear cell response. Deformation force curves of healthy and cancerous cells were processed according to the "brush on soft" cell model.[158] Results showed that healthy cells possess only one length of brush while cancerous ones display brushes with different lengths and densities. The results were in good agreement with the morphological characterization of the cells (Figure 9b). Indeed normal cells had a single-length brush and a grafting density of ≈2.4 μm and 300 molecules $\mu m^{-2}$, while cancerous cells had two brush lengths (0.45 and 2.6 μm) characterized by grafting densities of 640 and 180 molecules $\mu m^{-2}$, respectively (Figure 9c).

Recently, colloidal probes have offered an important tool to quantify the mechanical properties of cell in terms of its elasticity and viscosity. However due to their large size,

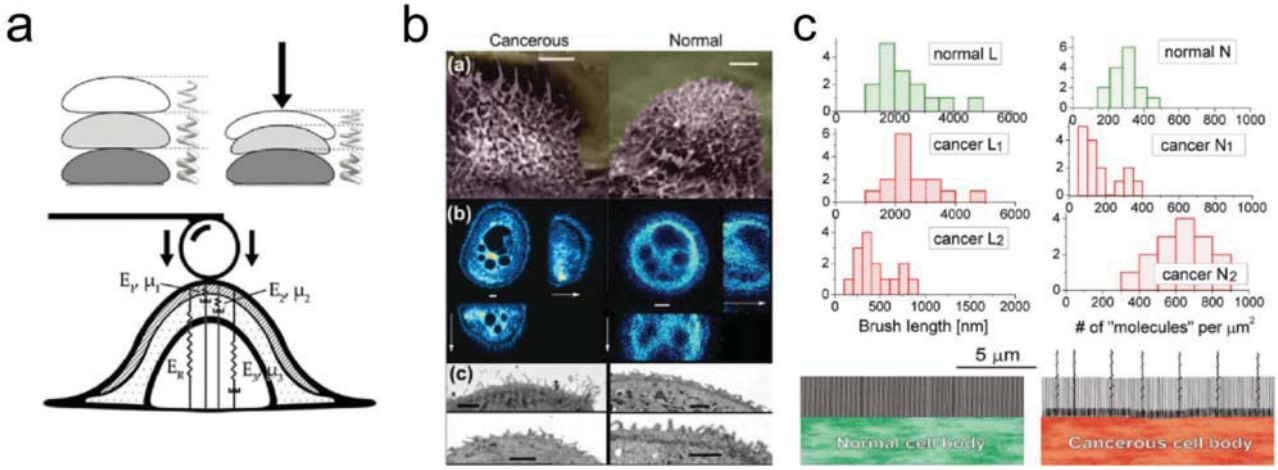


**Figure 9.** Colloidal probe-AFM. a) Schematics of the triple-layer structure before and after the application of load and generalized Maxwell model in which Young's modulus ($E$) and viscosity ($\mu$) are calculated for all the three compartments. Adapted with permission.[156] Copyright 2015, Elsevier Inc. b) SEM, confocal images and 3D cross-sections of cells showing the difference in brush density and length between cancerous and normal cells. c) Brush parameters obtained from force curves of normal and cancerous cells. Reproduced with permission.[158] Copyright 2011, Springer Nature.

direct mechanical characterization of small cellular compartments such as the nucleus and its membrane is difficult. To overcome that, the use of long, robust and thin probes that acts as nanoneedles has been proposed.[186] This particular approach has a specific advantage since it gives the possibility to create a nanoneedle able to penetrate the cell and to operate inside it without causing a substantial damage on the cell. CNTs grown or attached on the tip have also been used as sharp AFM probes for different purposes.[191–193] To date, CNT-modified tips, have been used to obtain high resolution images of the cell surface,[194] deliver cargo such as protein-coated QDs inside the cell,[195] and penetrate the cell nucleus.[196] Recently an interesting finite element analysis has been developed to describe the mechanical interactions between the cell and the CNT-AFM tip.[197] However, to the best of our knowledge, the use of CNT as nanoprobe to directly quantify the mechanical properties of the nucleus, for example, has not been achieved yet.

### *3.2.2. Optical Tweezers*

Optical tweezers (OT), introduced in 1986 by Ashkin et al.,[198] are a well-known optical trapping technique that can be used to investigate cell mechanical properties because it allows direct measurement of the forces acting on the cell membrane[164,199,200] and in the cytoplasm.[161,167] For the basic principles of the OT, please refer to ref. [201]. To study the mechanical properties of cells, particles that can be optically manipulated are either attached mechanically to the plasma membrane,[165,202] internalized in the cytoplasm,[161,167] or functionalized to target specific transmembrane proteins.[166,200,203] Then they are trapped and manipulated by light, and optical forces caused by the interaction between the probe and the cell are generated. To the best of our knowledge, NPs are not used as probes since their dimensions are often below the optical resolution and the forces that can be generated would be even more limited (very small), hence in the following section we will mainly discuss the use of microparticles in for the optical tweezers setup.

Cellular membrane properties and its mechanical interactions with the cytoskeleton have been investigated using OT-based membrane tether extraction.[199,200,202,204–206] In this experiment, an optically trapped microparticle (diameter range from 1 to 5 μm) is attached to the cell membrane and pulled away from the cell surface. The membrane attached to the particle deforms and creates a cylindrical extension, a tether (**Figure 10**a). Earlier studies by Hochmunt et al.[199] and Raucher and Sheetz[200] demonstrated that cells could create long tethers without increasing membrane tension because cellular membranes present a reservoir to buffer against mechanical deformations. Moreover, they observed that the adhesion between the cytoskeleton and membrane is finely regulated by plasma membrane phosphatidylinositol 4,5-bisphosphate.[204] Through investigation on the tether diameter and its mechanical resistance and length, the membrane mechanical behavior of stem cell and differentiated ones,[205] the effect of cholesterol on membrane viscoelasticity,[206] and the differences between several types of cells from the central nervous system[202] have been elucidated. Similarly, a recent study by Ayala et al.[165] revealed the influence of drugs (i.e., Blebbistatin, Cytochalasin D, and Jasplakinolide) on the F-actin cytoskeleton. By measuring the resistance of the tether and its radius, mechanical parameters of the membrane were extracted. Microrheology experiments were further performed by applying a sinusoidal displacement on a bead attached to the cell membrane. The viscoelastic response of the membrane-cytoskeleton complex was analyzed in terms of elastic and viscous modulus. The results showed that both tether mechanical properties and actin cytoskeleton depended on drug type and concentration; in particular all the three drugs destabilized the F-actin cytoskeleton and decreased the cell membrane tension.

Multiple optical tweezers can also be used simultaneously on a single cell to deliver an asymmetric stress and to study

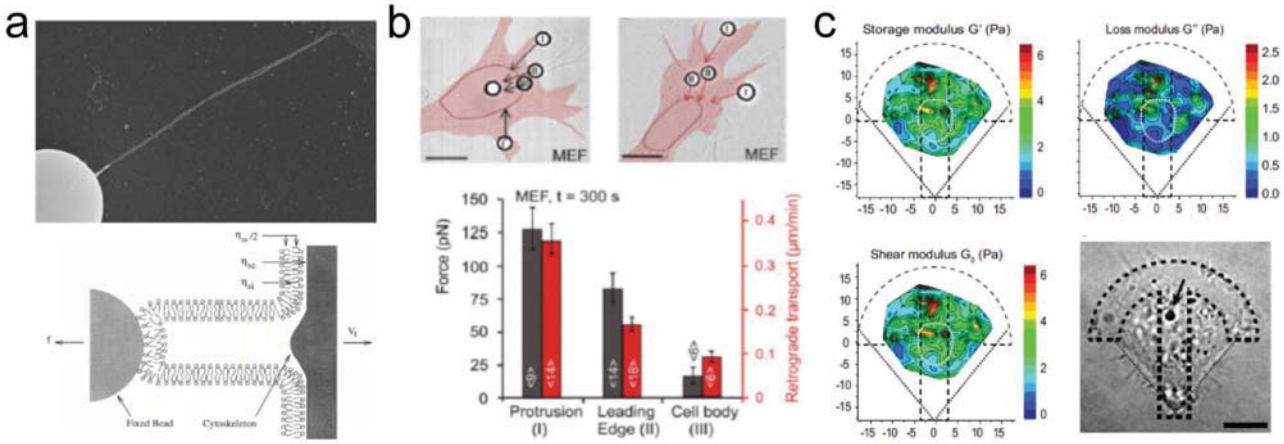


**Figure 10.** Application of optical tweezers for probing cell mechanics. a) SEM image (top) of a tether extracted from microglial cell treated with LPS (lipopolysaccharide) and (bottom) schematic of a tether being stretched at velocity $V_t$. Bottom: Adapted with permission.[199] Copyright 1996, The Biophysical Society. Top: Adapted with permission.[202] Copyright 2013, The Biophysical Society. b) Differential interference contrast images of fibronectin-coated beads adhering on cells in different positions. Black vectors denote CTF while red ones retrograde transport. The chart below depicts the dependence between forces and retrograde transport as a function of position on the cell ($n$ = 5). Adapted with permission.[166] Copyright the authors, published by Public Library of Science. c) Spatial distribution of storage, loss, and shear modulus and bright field image of cell adhering on a crossbow pattern; the shape of the pattern is highlighted by dotted lines. Adapted with permission.[167] Copyright 2016, National Academy of Sciences.

FA development and actomyosin regulated contractility.[203] Schwingel and Bastmeyer[166] for example, developed a multiple optical tweezers setup allowing the study the formation and maturation of FAs.[166] Up to 5 particles (with diameters of 3 and 4.5 μm) coated with fibronectin or RGD-peptides at different densities were adhered to the cell membrane. The force transmitted at the particle-FA interface depended on particle's properties and their spatial location on the membrane. Bead size, ligand type, and coating density affected force development; longer membrane protrusions and the leading edge generate higher forces and retrograde transport than the cell body (Figure 10b). The forces recorded on the protrusions were in the range of 100 pN while on the cell body they decreased to 15 pN. Interestingly it was observed that when the beads were close, the FAs coordinated and split the force among each other. Indeed CTF acting on single beads were reduced almost by half.

Mandal et al.[167] proposed a study to map intracellular mechanical properties by combining micropatterning and optical tweezers. Cells were first incubated with microparticles and then seeded onto crossbow-shaped adhesive patterns. Patterns were used to standardize the cellular shape and internal organization as well to quantify the spatial variation of mechanical properties. OT-based microrheology tests were performed by applying a step stress on the bead and by analyzing its displacement. Cell rheology was found to vary across the cells area. In particular, with this specific pattern, cells showed higher storage, loss and shear moduli in the center of the body (Figure 10c). The authors demonstrated the versatility of this setup by testing the effect of drugs and inhibitors on actin and microtubules and by analyzing the rheological differences between low and highly metastatic cells. Moreover, studying the impact of intracellular membranes on cell mechanics revealed a small contribution of these membranes on the shear modulus.

A combination of OT and AFM setup has been developed by Nawaz et al.[161] to study mechanical features of the cytoskeleton of 3T3 fibroblast cells at different indentation depths and loading rates. By using optical tweezers (indentation depth 0.2 μm, max force generated 10 pN), the mechanical response of the F-actin cytoskeleton was investigated and it was observed to be almost pure elastic and anisotropic. By employing AFM to increase the indentation depth and the loading forces (from 0.2 to 1 μm and from 10 to 600 pN, respectively) the authors observed a viscoelastic, rate dependent cell behavior. Indeed the apparent Young's modulus increased from ≈140 Pa to 330 Pa, increasing the indentation rate from 0.2 to 10 μm $s^{-1}$. They assumed that as soon as the cell is deeply indented, viscous intracellular elements, such as cytosol, the cell nucleus and the remodeling of the F-actin started influencing the mechanical response of the cell.

Although it has been used broadly to probe cell mechanics, this technique (OT) still possess substantial limitations, such as the utilization of high-powered lasers. This must be kept minimal to avoid local heating in the cell since this may alter cellular homeostasis.[20] However, this limits the forces generated by the OT to the pico-Newton range.[20] For this reason, optical tweezers are mainly employed to study the mechanics of smaller systems such as single molecules and proteins.[207]

### *3.2.3. Magnetic Manipulation*

Magnetic beads (MBs) such as iron oxide (e.g., magnetite and maghemite) or nickel and cobalt alloys NPs, microspheres, and rods offer the opportunity to introduce small and precisely located forces into specific cellular compartments[170,171,208,209] and surface receptors such as integrins and cadherin structures.[172,210–214] For this reason in the past years these materials have enabled the quantification of mechanical properties of the cytoplasm and nucleus,[171,208,209,215] and have been used to study mechanotransduction pathways.[168,172,213,216] MBs are thus extremely appealing due to some peculiar qualities that

distinguish them from other micro and NPs. When the beads are exposed to an external magnetic field (MF) they generate forces similar to the ones applied in vivo ($10^{-12}$ to $10^{-9}$ N). Moreover, they can be easily synthesized in a different sizes ranging from nanometers spherical particles to micrometer-beads and rods. Shape, crystallinity, and size uniformity are likewise fairly well controlled. MBs can be synthesized as single superparamagnetic NPs or multidomains ferromagnetic beads and their surface can be functionalized with specific ligands to target chosen receptors.

Based on their localization, the use of MBs as cell mechanics probes can be classified into two categories: MBs on the cell surface/membrane or intracellular MBs. It has been shown that ligand-coated MBs could target membrane receptors[172,210–212,214] such as cell–ECM and cell–cell adhesion receptors, whereas internalized MBs can be engineered to minimize their interaction with cytoplasmic structures,[171] or even to target specific sites inside the cells.[168]

MBs on the cellular membrane in the presence of magnetic field will stretch and mechanically activate the targeted membrane receptors. This technique is useful to study mechanotransduction as well as the rheological properties of cells.[215,217,218] Different types of forces can be applied on membrane-conjugated MBs (**Figure 11**): unidirectional tension delivered by the use of a permanent magnet (magnetic drag) or magnetic tweezers; torsional or rotational forces are applied by magnetic twisting/rotation.

In the first system (i.e., magnetic drag, Figure 11), it is possible to analyze the whole cellular response by performing biochemical assays. In the second case, magnetic tweezers generate a magnetic field gradient to pull single beads (Figure 11). This particular technique provides high spatial resolution, allows the manipulation of one MB at a time, and gives the possibility to follow its movement during the whole magnetic stimulation. The last type of force is magnetic twisting,[210] also called magnetic twisting cytometry, it is based on the rotation, or twist of premagnetized MBs in the direction of a MF and can be used to deliver torsional forces to single surface receptors.

The three mentioned forces have been used widely to study mechanotransduction at the single membrane receptor level and the relationship between surface transmembrane receptors and the cytoskeleton, in particular the structure and role of integrin in signaling.[210–212,214,219–221] Magnetic stimulation of integrin receptors has led to different responses, including local stiffening (reinforcement) due to actin accumulation in proximity of the FAs and cytoskeleton remodeling,[210] increase in tyrosine phosphorylation that mediate the FA formation,[219] endothelin-1 gene expression[222] and activation of mechanosensitive ion channels.[211,223,224] Moreover, Matthews et al.[214] studied the cellular response to static and dynamic integrin-mediated mechanical stimulation. They observed that bovine capillary endothelial cells use different mechanism to sense and respond to static and dynamic changes. For short stimulations, the cells showed a strengthening behavior dependent on the stiffening of adhesion structures (such as FA formation and F-actin cytoskeletal rearrangements). In contrast, when forces were applied over an extended time, cells rearranged their structures and retracted the stressed adhesions.[214]

The importance of other membrane receptors likes cadherin structures[172,225] and E-selectin[226] on cell mechanical behavior has been investigated as well. Marjoram et al.[172] proposed a new method to study mechanotransduction through the receptor protein VE-cadherin on HUVEC by combining magnetic drag and magnetic tweezers. By applying a permanent magnet, forces up to 200 pN (for 4.5 μm magnetic particles) were generated on the surface receptors. By performing several biochemical analyses (i.e., RhoGTPase activation, phosphotyrosine and adhesion complex analyses), they demonstrated that cells react to mechanical tension by activating RhoA, inhibiting Rac1 activity and increase the protein tyrosine phosphorylation level. By using the magnetic tweezers, a pulsatile force (40 pN for 2.8 μm MPs) was applied on single receptor-conjugated MBs. In this case it was noticed a

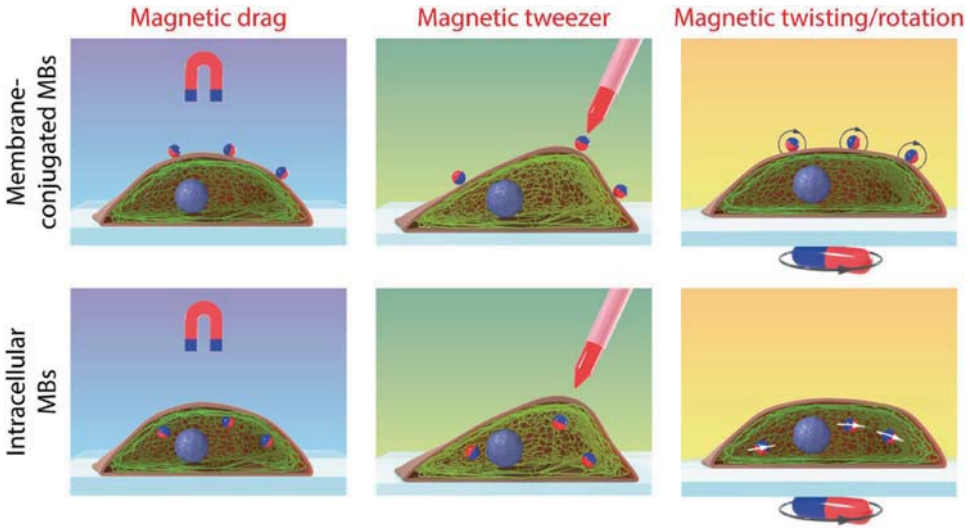


**Figure 11.** Schematic of magnetic-based mechanical stimulation techniques. MBs are conjugated to the cellular membrane or internalized in the cytoplasm. Afterward, forces on membrane receptors or intracellular compartments can be applied with static magnets (magnetic drag), magnetic tweezers or by magnetic twisting.

decrease in the particle displacement was associated with progressive local cellular stiffening induced by adhesion remodeling.[172] In addition, MBs are used to analyze mechanical pathways of internal cellular structures. Guilluy et al.[213] proposed an interesting work investigating the mechanotransduction of isolated nuclei. They mimicked the transmission of mechanical stress from the cytoskeleton to the nucleus by coupling 2.8 μm beads coated with anti-nesprin-1 antibody to nesprin-1, a linker of nucleoskeleton and cytoskeleton (LINC) complex. When nesprin-1 was subjected to a repeated mechanical stress, the bead displacement decreased indicating a stiffening of the nucleus. This behavior was found independent of chromatin and nuclear actin, and was uncorrelated to the RhoA activation pathway, which is observed during actin cytoskeleton remodeling. They claimed that a different mechanotransduction pathway related to LINC complex protein (emerin) and on lamin A/C was involved in regulation of nuclear stiffness.

It is important to mention that surface-bound MBs have also been used to elucidate the rheological behavior of cells, which has long been known to be dependent on cell lineage and experiment conditions. By applying dynamic magnetic twisting on RGD-coated MBs bounded on eukaryotic cells, four universal laws that describe cells mechanics have been extrapolated.[215,217] The laws are phenomenological and can be summarized as follows: (1) the frequency response of cells is scale free regardless the mechanical measurement technique; (2) cells are prestressed; (3) the diffusion of particles in the cytoplasm is anomalous; (4) stretch can significantly affect the rheology of cells.

In the case of intracellular MBs, MBs can be internalized either through cellular uptake pathway such as endocytosis or injected directly into the cells. Recent studies have demonstrated the use of internalized MBs to study mechanotransduction pathways[168,170] and the elastic and viscoelastic properties of the cytoplasm and nucleus (**Figure 12**).[171,208,209]

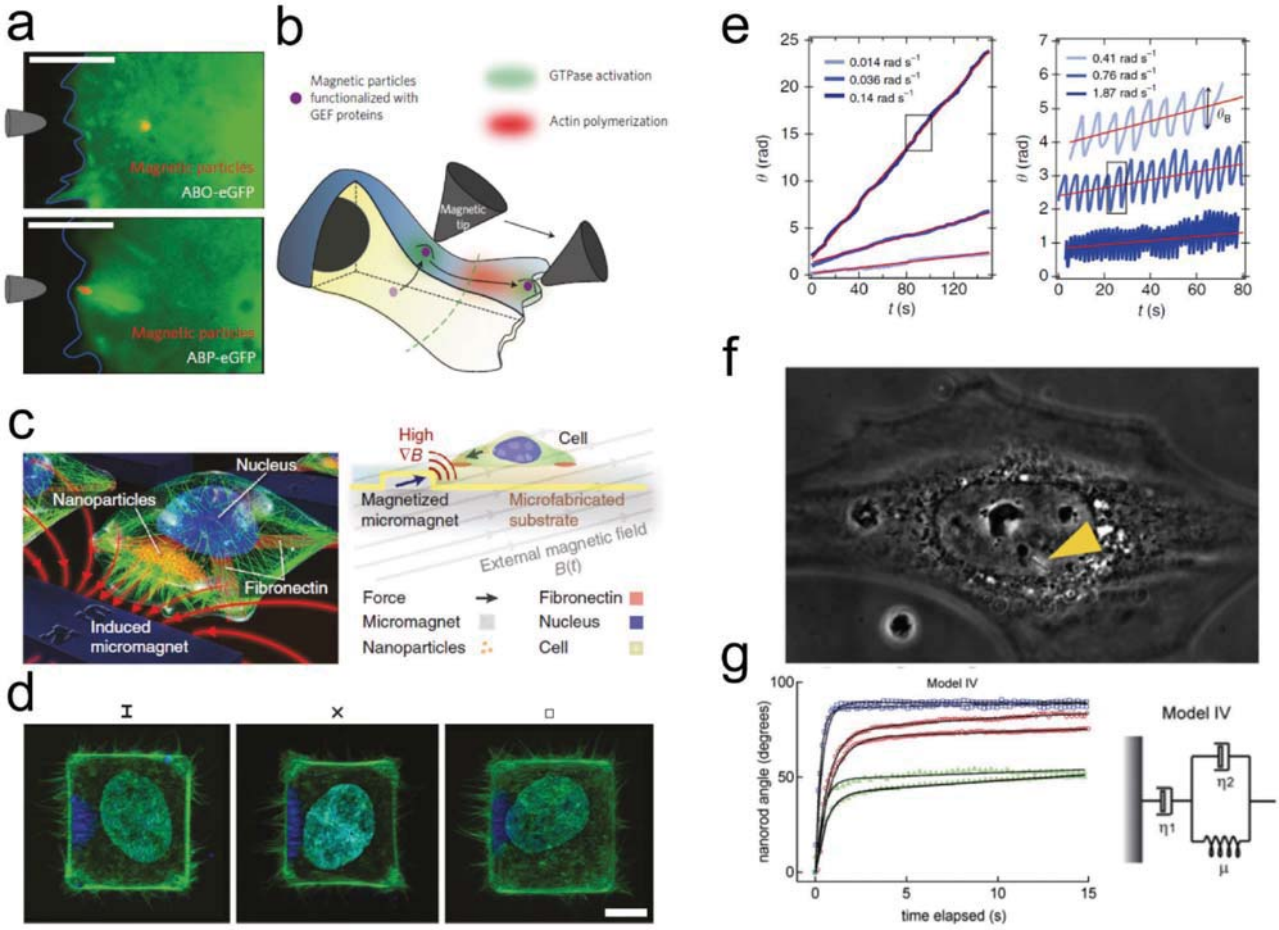


**Figure 12.** a) Functionalized NPs (red) in the cell body (top) and creating an actin cloud (bottom). b) Scheme illustrating the dependence of actin polymerization on the NPs localization. Adapted with permission.[168] Copyright 2013, Macmillan Publishing. c) Schematics of the micropatterned magnetic platform. d) Confocal images of F-actin polymerization (green) in cells adhering on different patterns (line: I; cross: X; square: □). Adapted with permission.[170] Copyright 2012, Nature Springer. e) Evidence of frequency-dependent wire instability in cells: for rotational frequency lower than the critical frequency, the wires can rotate inside the cells. For frequency higher than the critical frequency, the wires oscillate in the cytoplasm. Reproduced with permission.[171] Copyright 2016, Springer Nature. f) Bright-field image of a nanowire located in the cell nucleus. g) Time-dependent rotations of normal cell (green), deficient lamin A/C deficient cell (red) and cytoplasm (blue) and the corresponding fits (black lines) obtained with the represented spring-dashpot model. Adapted with permission.[209] Copyright 2011, The Biophysical Society.

Etoc et al.,[168] as the first example, used magnetic NPs (MNPs) embedded in the cytoplasm as a signaling platforms to trigger the Rho-GTPases transduction pathway, a series of signaling proteins known to regulate cell morphology through intracellular actin cytoskeleton remodeling.[227] To improve the functionalization and the colloidal stability of MNPs, the proteins of interest were coupled to the MNPs directly in the cytoplasm. They demonstrated that actin polymerization and the activation of Rac1 were both dependent on the presence and location of functionalized MNPs. In particular, Rac1 was triggered by magnetically driving the nanoparticles functionalized with guanine nucleotide exchange factors proteins close to the cellular membrane (Figure 12a) and did not occur when the particles were embedded in the cytosol far from the membrane. Moreover, Rac1 activation occurred everywhere near the membrane while actin polymerization only happened where functionalized MNPs were located in proximity of protrusive areas (Figure 12b). This work demonstrated the possibility to magnetically manipulate cell signaling from inside the cytoplasm using specific functionalized MNPs and could be theoretically applied to other systems.[168]

In order to produce statistically relevant results by reducing the uncertainties related to a single cell experiments, Tseng et al.[170] developed a multicellular magnetic platform to provide mechanical stimulation to thousands of cells simultaneously. The authors designed a substrate with an array of soft magnetic elements located in the proximity of fibronectin coated patterns. HeLa cells were loaded with fluorescent MNPs and subsequently seeded on the patterned substrate. Once the cells adhered to the substrates, the soft ferromagnetic elements were carefully magnetized and the internalized NPs induced unidirectional forces on the cellular cortex (Figure 12c). It was observed that F-actin polymerization and asymmetry were strongly related to NP-induced tension (Figure 12d) and depended on the synergistic effect between the load of particles in the cells, the fibronectin pattern, and the applied magnetic force. Moreover, using a similar system the authors investigated other biomechanical parameters such as the role of protein p21-activated kinase in MBs-mediated filopodia generation and the effect of MBs during mitosis.

Aside from studying internal biochemical pathways, MB-assisted mechanical stimulation has been used to study the elastic and viscoelastic behavior of cytoplasm and nucleus for example, using spherical beads[218] and microrods.[171,208,209] When magnetic rods and wires are embedded in the cells and are subjected to a rotational magnetic field they behave as microrheometers. Therefore, from the rod's rotation, it is possible to retrieve mechanical parameters of the cellular compartments.[171,208,209] Recent progresses in the study of the rheology of cytoplasm are represented by the work of Berret.[171] By applying the rotational magnetic spectroscopy technique, he monitored the wire's rotational instability in living cells in order to further understand whether the cytoplasm possessed an elastic gel or viscoelastic liquid-like behavior. Superparamagnetic microwires (diameter and median length ≈0.5 and 2.4 μm) were injected in the cytoplasm and subjected to a rotating MF at different frequencies (from 0.014 to 1.87 rad $s^{-1}$). At low frequency, the wires rotated freely inside the cytoplasm, however, when the frequency was increased, the wires developed a rotational instability oscillating "back and forth" (Figure 12e). By analyzing the trajectory of the rods and the frequency at which transition from full rotation to oscillation occurs, the author modelled the cytoplasm as a viscoelastic fluid. This result is novel since so far, the cytoplasm has been described as an elastic gel.[208] However, a conclusive answer on the mechanical nature of cytoplasm is still unclear and the observed differences among results can be related to experimental parameters (i.e., cell line, material functionalization and size, MF strength, and rotation frequency).

More specific investigations into the viscoelastic behavior of the nucleus were performed by Celedon et al.[209] Magnetic nanorods made from platinum and nickel composite (diameter 200 nm and length 2.5 μm) were injected in the nuclei of wild-type mouse embryonic fibroblast cells (Figure 12f). Creep experiments were performed applying a rotational force on the nanorods and by analyzing the residual angle between the nanorod axis and the MF direction. Shear modulus and viscosity were analyzed by modeling the time evolution of the residual angle with a viscoelastic spring-dashpot model (Figure 12g). In particular, it was observed that the nucleus presents a significant elastic component. Moreover, by analyzing lamin A/C deficient cells the authors observed a decrease in viscosity and shear modulus, therefore corroborating the hypothesis that nucleus viscoelasticity depends on the integrity of lamin A/C.

Apart from using MBs for single cell experiments, magneto-mechanical stimulation has been further implemented on a larger scale to investigate the biomechanics of 3D microtissues.[228–230] Magnetic microtissue systems are comprised of collagen microgel-based tissues tethered between two elastomeric micropillars. Magnetic forces (≈100 μN) can be applied on a magnetic bead placed on top of the pillar. Cell contractile forces are quantified by observing the bending of the poles while magnetic actuation on the bead allows evaluation of the microtissue's overall stiffness. These systems have permitted the separation of the contributions from cells and matrix,[228] can be used for long term studies[229] and have been recently adapted to perform simultaneous stimulation on a multiple microtissues.[230]

Overall, MBs have been an extremely useful tool to study mechanotransduction and biomechanics. Their key strength, if compared to other techniques such as OT and AFM, is the possibility to apply well controlled forces to specific cellular regions and receptors in a noninvasive way. However, in order to employ this technique to further answer biologically related questions, a more careful design and characterization of MBs is required. More specifically, to study the mechanical properties of cells and the nucleus it is necessary to verify the state of MBs inside the investigated cellular compartment in order to guarantee that the MBs surface functionalization does not entangle the MBs in cytoplasmic or nuclear structures. Furthermore, for nanometer-sized probes, it is advisable to deeply investigate the state of the MNPs in the cell compartments since their integrity, colloidal stability, magnetic behavior and crystallinity could be impaired by cellular internalization. Finally, it must be verified that the presence of the MBs in the cells or on its surface does not influence cells mechanics.

#### 3.2.4. Particle Tracking Microrheology

Particle tracking microrheology (PTM) is a passive technique used to measure the viscoelastic properties of cytoplasm. This technique was introduced by Tseng et al.[231] in 2002 and has since become a popular tool allowing the measurement of cytoplasmic properties noninvasively in 2D substrates, 3D matrices, and under shear flow conditions with high spatial and temporal resolution.[232] Even though intracellular organelles such as granules,[233] mitochondria,[234] and peroxisomes[235] can be used as trackers, fluorescent polystyrene micro or NPs are more commonly used. The particles are ballistically injected or internalized in the cytoplasm. The ballistic transfer of beads to the cytoplasm is performed by spreading the beads on a grid placed in an injection device. By applying pressure drop on top of the grid, the beads are bombarded into the cells.[236] Afterward bead motion is tracked with time-lapse optical microscopy. From the recorded movement of the particles it is possible to retrieve the elastic and viscoelastic properties of the cytoplasm. For a detailed description of PTM and its basic principles we suggest a comprehensive review from Wirtz.[232]

From its first implementation,[231] PTM has been used to investigate several mechanical aspects of the cells. This technique helps to study how the cells react to different external stimulation such as shear stress,[237,238] temperature, and pH.[239] Moreover, PTM has been used to quantify the rheology of cells in 3D matrixes,[240] the influence of X-ray irradiation on the mechanics of healthy and tumor cells[241] and the effect of transforming growth factor-$\beta$1 (TGF-$\beta$1) on mechanical and structural properties of murine MSCs.[174] Furthermore, physiological processes like cells differentiation[173,242] and cell division, i.e., mitosis[173] can be monitored using this technique. Chen et al.[175] induced osteogenic and adipogenic differentiation of human mesenchymal stem cells (hMSCs) and observed how mechanical parameters vary during the process and correlated the changes with morphological and biochemical parameters. In particular, they noticed that osteogenic differentiation resulted in a rise in the storage and loss modulus (parameters that describe elastic and viscous behavior, respectively) together with an increase of FA sites and rearrangement of the actin cytoskeleton. Conversely, adipogenic differentiation led to a decrease in elastic and viscoelastic properties. In this case, the cytoplasm maintained a fluid-like behavior. The rheological behavior of HeLa cells undergoing mitosis was investigated by Chen et al.[173] Both elastic and viscoelastic moduli (in rheology experiments expressed as $G'(f)$, $G''(f)$) were observed to increase from metaphase ($G'(f)$: ≈2.5 Pa; $G''(f)$: 2.5 Pa) to anaphase ($G'(f)$: ≈5–10 Pa; $G''(f)$: 12.5 Pa) and stabilized to a constant during telophase. In this work, the authors correlated the increase of viscosity with a rise in microtubules density.

One of the advantages of PTM is the ability to probe different systems at the same time. Panzetta et al.[176] recently analyzed the mechanical properties of both cells and the ECM simultaneously. First, biopsies of healthy and cancerous lung tissue were obtained for 10 different patients. Then 500 nm carboxylated fluorescent polystyrene particles were introduced in the tissues. Tracking the particles in the ECM and in the cells ex vivo helped to evaluate the synergy between the ECM and the cells. Interestingly, it was observed that in unhealthy biopsies, the cells became 3.5 times more compliant and matrix stiffening decreased particle mobility ≈4 fold.

In general, particle tracking microrheology appears to be a powerful method to study the mechanical properties of cells without interacting directly with them. Moreover, this technique, when applied simultaneously on the cells and ECM-like environment, may help to determine the relation between the ECM and cells in healthy and cancerous systems (on 2D substrates and in more complex systems such as 3D scaffolds). Nevertheless, PTM experiments over a prolonged time require investigation into cellular adaptation (i.e., to study the effect of substrate stiffness or degradation on cells adhesion and spreading), and the colloidal and fluorescent stability of the particles in the cytoplasm.

### 3.3. Summary and Outlook for Particles as a Tool to Measure Cell Mechanics

Size, geometry, surface functionalization and size specific properties (i.e., superparamagnetism, plasmonic properties) of micro and NPs make these systems attractive because they can interface at a subcellular level. For these reasons, micro and NPs can be used as probes to investigate the biomechanics of cell and mechanotransduction pathways. In this regard, **Table 2** and Section 3.3.1 ffer a schematic summary of key articles where micro and NPs are applied to study cell mechanics. This field is open and continuously evolving: To further improve its general knowledge we believe in the necessity of improving all aspects of cell mechanics measurements. Together with the development of higher performance platforms (e.g., microscopes with higher spatial and temporal resolution), improving the testing probes (micro and NPs) is also necessary. Here, a better understanding of the stability of particles outside and inside cells is fundamental to validate the experimental setup and therefore the results. In applications such as OT, magnetic manipulation and PTM, internalized particles should maintain their chemical integrity (i.e., they do not decompose nor dissolve), their crystalline phase, their fluorescence, their colloidal stability, and should not interact with intracellular compartments (unless appropriately designed to do so). In addition, the full potential of NPs to study cell mechanics has not yet been explored. First, stimuli-responsive substrates incorporating NPs such as SPIONs and plasmonic NPs could be used to study biomechanical cellular response to cyclic mechanical stimulations (i.e., FA formation and maturation kinetics). Small and bright probes such as QDs or carbon dots could be systematically inserted into substrates for TFM to improve the CTF field reconstruction. Finally, AFM tips decorated with robust CNTs could be valuable probes to directly investigate the mechanical properties of internal cell compartments (i.e., the nucleus and nuclear membrane) without impairing the cell integrity. The number of studies that potentially can be carried out is seemingly endless and will only be limited by the quality of the materials, the optics resolution and by the robustness of biophysical models.

**Table 2.** Application of particles for the biomechanical characterization of cells.

| Particle type | Particle size and coating | Application | Cell type | Relevant information obtained from the experiments | Ref. |
|---|---|---|---|---|---|
| AuNPs | <8 nm cRGD | Nanopatterned substrates | Rat embryonic fibroblasts | Substrates with dual functionalization improve cell attachment, FA assembly and spreading | [117] |
| | Aminoalkyl thiol moleculess | Nanopatterned substrates | PRCN | The increase in NPs density promotes cell viability and neurite development | [118] |
| | 8 nm cRGD | Nanopatterned substrates | Rat embryonic fibroblasts | Substrates with different stiffness and same functionalization (NPs density) influence differently the cells: on softer substrates cells can adhere even at low NPs density | [126] |
| Ferromagnetic beads | Diameter: 4.5 μm RGD-peptide | Magnetic manipulation | HASM, HLF, HBE and MDCK cells | Cells mechanical behavior can be summarized in four universal laws applicable to all type of eukaryotic cells | [215] |
| Magnetic beads | Diameter: 4.5 μm | Magnetoresponsive substrates | human fibroblasts | Upon the application of a static field the substrates increase their stiffness and the cells increase of 30% their adhesion area; with the application of a oscillatory field the cells migrate due to pulsatile surface translocation | [136] |
| | Diameter: 2.8 μm Anti-nesprin-1 | Magnetic manipulation | HeLa, HUVEC, and MRC5 cells | Emerin, a LINC complex protein and lamin A/C are involved in the regulation of the nuclear stiffness | [213] |
| MNPs | Diameter: 480 ± 110 nm Cdc42Q61L GEF proteins | Magnetic manipulation | NIH3T3 fibroblasts and cos7 cells | MNPs are internalized and trigger the Rho-GTPases transduction pathways from inside the cytoplasm | [168] |
| | Dextran fluorescent (red) | Magnetic manipulation | HeLa cells | F-actin polymerization, cytoskeleton asymmetry and mitotic spindle orientation are influenced by MNPs induced forces | [170] |
| Nickel beads | Diameter: 100 μm | Magnetic manipulation | NIH3T3 fibroblasts | Cell and ECM both contribute to the biomechanics of 3D microtissues. | [228] |
| Nickel–platinum rods | Length: 2.5 μm Diameter: 200 nm | Magnetic manipulation | Wild-type mouse embryonic fibroblast cells | Nucleus viscoelasticity is influenced by the state of lamin A/C: in lamin A/C deficient cells, nucleus viscosity and shear modulus are decreased | [209] |
| Nickel wires | Length: 20 μm | Magnetoresponsive substrate | A7R5 rat smooth muscle cells | Cells respond immediately to roughness changes changing their adhesion area but cells area is not influenced by long-term oscillation | [134] |
| Polystyrene beads | 0.2 μm fluorescent (yellow) | TFM | Mouse embryo fibroblasts | Observation of CTF field in 3D: out-of-plane rotational moments are sustained by the FAs on retracting and protruding regions | [150] |
| | 40 nm fluorescent (red) | TFM | RBL-2H3 rat basophilic leukemia cells | Implement of STED in TFM to increase the optical resolution and the CTF field reconstruction | [152] |
| | 0.5 μm carboxylate fluorescent (yellow, red) | TFM | Physarum amoebae | By distributing the fluorescent beads in two separate gel layers it is possible to quantify the Poisson's ratio during TFM experiments | [151] |
| | 200 nm carboxylate fluorescent (red, green) | TFM | HuO9 human osteosarcoma cells | Development of a simulation platform to optimize the TFM experiments | [154] |
| | Diameter: 3.0 μm | OT | NIH3T3 fibroblasts | Tether extraction experiments and rheology measures are used to quantify the effects of drugs on the membrane-cytoskeleton complex: Blebbistatin, Cytochalasin D, and Jasplakinolide destabilize the cytoskeleton and decrease the cell membrane tension | [165] |
| | Diameter: 3.0 and 4.5 μm Carboxylate FN and cRGD | OT | Mouse B16F1 melanoma cells | With a multiple OT setup FAs formation and maturation is studied: (1) bead size, ligand type, and coating density affect force development; (2) forces are distributed anisotropically on the cell | [166] |
| | Diameter: 2.0 μm fluorescent (red) | OT | RPE-1, MCF-10A, and MDA-MB-231 cells | Mapping of the cell microrheology reveals differences in cell storage, loss, and shear moduli across the cell body | [167] |
| | Diameter: 0.76 μm | OT | 3T3 mouse embryonic fibroblasts | For loading forces of 10 pN the response of the F-actin cytoskeleton is pure elastic and anisotropic | [161] |
| | Diameter: 1.98 μm | AFM | 3T3 mouse embryonic fibroblasts | For loading forces up to 600 N the cell behaves as a viscoelastic system | [161] |

**Table 2.** Continued.

| Particle type | Particle size and coating | Application | Cell type | Relevant information obtained from the experiments | Ref. |
|---|---|---|---|---|---|
| | Diameter: 200 nm carboxylated, fluorescent (red) | PTM | hMSCs | Elasticity and viscosity of cells increase during osteogenic differentiation and decrease during adipogenic differentiation | [175] |
| | Diameter: 100 nm carboxylated, fluorescent (red) | PTM | HeLa cells | The elastic and viscoelastic moduli vary when the cell undergoes mitosis: both moduli increase from metaphase to anaphase and stabilize during telophase | [173] |
| | Diameter: 500 nm carboxylated | PTM | Biopsy tissues from human lungs | In adenocarcinoma biopsies the cells are softer (3.5 times) and the ECM is stiffer (4 times) than for healthy biopsies | [176] |
| QDs (CdSe–CdS–ZnS) | >4.1 nm fluorescent (blue, green, red) | TFM | HeLa cells, embryonic fibroblasts, HUVEC, MCF10A, and PC12 cells | QDs incorporated in fluorescent nanodisks allow to increase the spatial resolution, the CFT reconstruction on the FA and to record in and out-of-plane CTFs | [153] |
| Silicon wires | Length: 5–10 μm diameter: 40 nm FN | Nanopatterned substrate | Primary normal human dermal foreskin fibroblasts | Cells adhesion, spreading and division depend on the dynamics of the contact angle created between the filopodia and the substrate | [116] |
| $SiO_2$ beads | Diameter: 10 μm | Colloidal probe AFM | MCF10A and MDA-MB-321 breast cells | Cellular subdomains become stiffer and more viscous with depth. Metastatic cells are softer than noninvasive ones | [156] |
| | Diameter: 5 μm | Colloidal probe AFM | Human cervical epithelial cells | Colloidal probe AFM combined with a "brush on soft" cell model reveal surface structural differences in the cells: healthy cells show a single compact layer for uniform microvilli while cancerous ones display microvilli with different lengths and densities | [158] |
| Superparamagnetic beads | Diameter: 4.5 μm RGD-peptide nonintegrin activating anti-$\beta$1 antibody | Magnetic manipulation | Bovine capillary endothelial cells | Integrins respond differently to static and dynamic mechanical stimulation: for short stimulations FA are formed and the cytoskeleton rearranges; for dynamic stimulations the cell remodels | [214] |
| | Diameter: 2.8 and 4.5 μm hVEC-Fc | Magnetic manipulation | HUVEC | Mechanical stimulation of VE-cadherins induces RhoA activation, Rac1 inhibition, an increase in tyrosine phosphorylation level and local stiffening and remodeling around the VE-cadherin | [172] |
| Superparamagnetic wires | Length: 0.5–2.4 μm | Magnetic manipulation | NIH3T3 fibroblasts and HeLa cells | By rotating and oscillating the rods inside the cells, the cytoplasm is described as a viscoelastic fluid | [171] |



### *3.3.1. Take-Home Messages*

- Functionalized NPs adhering on substrates can be used to study ECM-cell adhesion in terms of ECM ligands density,[114,115] ligand type,[117] and FA dynamics.[116]
- Dynamic substrates with variable stiffness and topography can be synthesized using responsive NPs (i.e., magnetic NPs).[134,136] These substrates provide a versatile platform to mimic cells response to the mechanical variations in the ECM.
- Particles incorporated in soft substrates are used in traction force microscopy to study the forces generated by cells. By varying particles density, distribution and position in the substrates, it is possible to improve the force reconstruction process.[153,154]
- AFM tips can be modified with microbeads. The increase in the contact area between the probe and the cell membrane lowers the possibility to damage cells, smooths local variations and simplifies the contact geometry. The modified tips help to study intracellular compartments[156] and complex cell surface geometries.[158]
- Elasticity and viscosity of the cell membrane and of the cytoplasm can be estimated in situ with optical tweezers. Moreover, multiple optical tweezers can be used simultaneously to deliver asymmetric stresses on FA[166] and to map the intracellular rheological behavior.[167]
- With magnetic beads, forces in the physiological range are delivered to specific location on the cell membrane and to intracellular compartments. By applying static and rotational magnetic fields, mechanotransduction pathways[168,170] and cells mechanical properties[171,215] have been elucidated.
- Particle tracking microscopy is a noninvasive technique that allows the mechanical characterization of cell compartments in complex environments (e.g., under shear flow or in a 3D matrix) and during physiological processes as cell division and differentiation.[173,175] Moreover this technique can be expanded to test ECM rheology.[176]

## 4. Final Conclusions and Outlook

Bionanomechanics is intended to complete our general understanding in the field of (micro and nano) particle–cell interaction. This field covers two major interconnected aspects: The influence of NP on cell mechanics (i.e., cell adhesion, cytoskeleton, cell stiffness, and migratory property of the cells) and the application of particles to probe cell mechanics, including rheological properties and mechanotransduction pathways. Regarding the impact of NPs on cell mechanics, the destruction of cellular barriers (e.g., tight junctions), reduction of cell–ECM adhesion, the formation of aberrant F-actins and MT, an increase in cell stiffness, and retardation of cell migration was observed for cells exposed to NPs. However, there is an urgent need to thoroughly study the influence of NPs on cell mechanics with NPs acting at subcytotoxic concentrations. Second, these advances in understanding will be aided by the utilization of particles as probes to directly and more precisely evaluate these cellular phenomena.

Further progress in this field will build on fundamental insights and the application of intracellular and extracellular particles to alter/probe cell mechanics. Many aspects have not yet been explored, such as how NPs influence IF, NP, physicochemical property–cell mechanics relationships, and mechanotransduction in the presence of NPs to name some. The development of novel dynamic substrates and detection systems for measuring CTF could help elucidate the transmission and translation process of this cellular nanoscale force, while development of compartment-specific targeting particles will help to describe rheological properties of each targeted organelles/structures. Moreover, particle-based techniques could be systematically used to quantify the effect of internalized NPs on cell mechanics: TFM could be implemented to study NPs-induced variations on the CTF field, while colloidal probe AFM, OT, and PTM could be used to study how NPs affect the viscoelasticity of the cell and its compartments. Nevertheless it is important to underline that cell elasticity and viscosity are useful parameters for comparison between different experimental conditions, but caution must be applied when interpreting the results as absolute values. Indeed the mechanical models used to fit experimental results do not completely grasp the biomechanical complexity of cellular rheology. Advanced models have been proposed, however a unified mechanistic theory has not been elaborated yet.


## Acknowledgements

D.S., F.C., and T.L.M. contributed equally to this work. The authors would like to acknowledge the Swiss National Science Foundation, through the National Center of Competence in Research Bio-Inspired Materials and the Adolphe Merkle Foundation for financial support of the project. The authors kindly thank Dr. Miguel Spuch Calvar for graphical design.


## Conflict of Interest

The authors declare no conflict of interest.


## Keywords

bionanomechanics, cell mechanics, microparticles, nanoparticles

Received: August 8, 2017
Revised: September 14, 2017
Published online:



[1] A. E. Nel, L. Mädler, D. Velegol, T. Xia, E. M. V Hoek, P. Somasundaran, F. Klaessig, V. Castranova, M. Thompson, *Nat. Mater.* **2009**, *8*, 543.
[2] A. Verma, F. Stellacci, *Small* **2010**, *6*, 12.
[3] L. Shang, K. Nienhaus, G. U. Nienhaus, *J. Nanobiotechnol.* **2014**, *12*, 5.
[4] Y. Jiang, S. Huo, T. Mizuhara, R. Das, Y. Lee, S. Hou, D. F. Moyano, B. Duncan, X. Liang, V. M. Rotello, *ACS Nano* **2015**, *9*, 9986.
[5] B. D. Chithrani, A. A. Ghazani, W. C. W. Chan, *Nano Lett.* **2006**, *6*, 662.
[6] R. Agarwal, V. Singh, P. Jurney, L. Shi, S. V. Sreenivasan, K. Roy, *Proc. Natl. Acad. Sci. USA* **2013**, *110*, 17247.
[7] S. Tenzer, D. Docter, J. Kuharev, A. Musyanovych, V. Fetz, R. Hecht, F. Schlenk, D. Fischer, K. Kiouptsi, C. Reinhardt, K. Landfester, H. Schild, M. Maskos, S. K. Knauer, R. H. Stauber, *Nat. Nanotechnol.* **2013**, *8*, 772.
[8] M. Lundqvist, J. Stigler, G. Elia, I. Lynch, T. Cedervall, K. A. Dawson, *Proc. Natl. Acad. Sci. USA* **2008**, *105*, 14265.
[9] G. Bao, S. Suresh, *Nat. Mater.* **2003**, *2*, 715.
[10] D. A. Fletcher, R. D. Mullins, *Nature* **2010**, *463*, 485.
[11] D. E. Discher, P. Janmey, Y.-L. Wang, *Science* **2005**, *310*, 1139.
[12] S. Harada, G. A. Rodan, *Nature* **2003**, *423*, 349.
[13] C. M. Lo, H. B. Wang, M. Dembo, Y. L. Wang, *Biophys. J.* **2000**, *79*, 144.
[14] A. J. Engler, S. Sen, H. L. Sweeney, D. E. Discher, *Cell* **2006**, *126*, 677.
[15] C. Rotsch, F. Braet, E. Wisse, M. Radmacher, *Cell Biol. Int.* **1997**, *21*, 685.
[16] C. Rotsch, M. Radmacher, *Biophys. J.* **2000**, *78*, 520.
[17] T. K. Berdyyeva, C. D. Woodworth, I. Sokolov, *Phys. Med. Biol.* **2005**, *50*, 81.
[18] Q. S. Li, G. Y. H. Lee, C. N. Ong, C. T. Lim, *Biochem. Biophys. Res. Commun.* **2008**, *374*, 609.
[19] I. Sokolov, S. Iyer, C. D. Woodworth, *Nanomed. Nanotechnol., Biol. Med.* **2006**, *2*, 31.
[20] E. Moeendarbary, A. R. Harris, *WIREs Syst. Biol. Med.* **2014**, *6*, 371.
[21] D. E. Ingber, *Ann. Med.* **2003**, *35*, 564.
[22] C. P. Heisenberg, Y. Bellaïche, *Cell* **2013**, *153*, 948.
[23] J. H. Shawky, L. A. Davidson, *Dev. Biol.* **2015**, *401*, 152.
[24] M. S. Steinberg, M. Takeichi, *Proc. Natl. Acad. Sci. USA* **1994**, *91*, 206.
[25] M. Prager-Khoutorsky, A. Lichtenstein, R. Krishnan, K. Rajendran, A. Mayo, Z. Kam, B. Geiger, A. D. Bershadsky, *Nat. Cell Biol.* **2011**, *13*, 1457.
[26] A. Zemel, F. Rehfeldt, A. E. X. Brown, D. E. Discher, S. A. Safran, *Nat. Phys.* **2010**, *6*, 468.
[27] S. J. Han, K. S. Bielawski, L. H. Ting, M. L. Rodriguez, N. J. Sniadecki, *Biophys. J.* **2012**, *103*, 640.
[28] C. S. Ranucci, P. V. Moghe, *J. Biomed. Mater. Res.* **2001**, *54*, 149.
[29] E. K. F. Yim, E. M. Darling, K. Kulangara, F. Guilak, K. W. Leong, *Biomaterials* **2010**, *31*, 1299.
[30] T. Wang, J. Bai, X. Jiang, G. U. Nienhaus, *ACS Nano* **2012**, *6*, 1251.
[31] X. Jiang, C. Rocker, M. Hafner, S. Brandholt, R. M. Dorlich, G. U. Nienhaus, *ACS Nano* **2010**, *4*, 6787.
[32] B. Yameen, W. I. Choi, C. Vilos, A. Swami, J. Shi, O. C. Farokhzad, *J. Controlled Release* **2014**, *190*, 485.

[33] C. R. Keese, I. Giaever, *Exp. Cell Res.* **1991**, *195*, 528.
[34] V. Saravia, J. L. Toca-Herrera, *Microsc. Res. Tech.* **2009**, *12*, 957.
[35] B. Alberts, D. Bray, J. Lewis, M. Raff, K. Roberts, J. D. Watson, *Molecular Biology of the Cell Second Edition.*, Garland Publishing, New York **1989**.
[36] A. A. Khalili, M. R. Ahmad, *Int. J. Mol. Sci.* **2015**, *16*, 18149.
[37] L. Xu, M. Dan, A. Shao, X. Cheng, C. Zhang, R. A. Ayokel, T. Takemura, N. Hanagata, M. Niwa, D. Watanabe, *Int. J. Nanomed.* **2015**, *10*, 6105.
[38] M. I. Setyawati, C. Y. Tay, S. L. Chia, S. L. Goh, W. Fang, M. J. Neo, H. C. Chong, S. M. Tan, S. C. J. Loo, K. W. Ng, J. P. Xie, C. N. Ong, N. S. Tan, D. T. Leong, *Nat. Commun.* **2013**, *4*, 1673.
[39] Y.-M. Long, X.-C. Zhao, A. C. Clermont, Q.-F. Zhou, Q. Liu, E. P. Feener, B. Yan, G.-B. Jiang, *Nanotoxicology* **2015**, *5390*, 1.
[40] M. I. Cybulsky, M. A. Gimbrone, *Science* **1991**, *251*, 788.
[41] R. G. Collins, R. Velji, N. V. Guevara, M. J. Hicks, L. Chan, A. L. Beaudet, *J. Exp. Med.* **2000**, *191*, 189.
[42] Z. M. Dong, S. M. Chapman, A. A. Brown, P. S. Frenette, R. O. Hynes, D. D. Wagner, *J. Clin. Invest.* **1998**, *102*, 145.
[43] E. G. Nabel, *Am. J. Cardiol.* **1991**, *68*, 6.
[44] E. Oesterling, N. Chopra, V. Gavalas, X. Arzuaga, E. J. Lim, R. Sultana, D. A. Butterfield, L. Bachas, B. Hennig, *Toxicol. Lett.* **2008**, *178*, 160.
[45] S. J. H. Soenen, N. Nuytten, S. F. De Meyer, S. C. De Smedt, M. De Cuyper, *Small* **2010**, *6*, 832.
[46] X. Zhao, J.-L. Guan, *Adv. Drug Delivery Rev.* **2011**, *63*, 610.
[47] Y. Hou, K. Cai, J. Li, X. Chen, M. Lai, Y. Hu, Z. Luo, X. Ding, D. Xu, *Int. J. Nanomed.* **2013**, *8*, 3619.
[48] X. Wu, Y. Tan, H. Mao, M. Zhang, *Int. J. Nanomed.* **2010**, *5*, 385.
[49] C. Y. Tay, P. Cai, M. I. Setyawati, W. Fang, L. P. Tan, C. H. L. Hong, X. Chen, D. T. Leong, *Nano Lett.* **2014**, *14*, 83.
[50] L. Saldaña, N. Vilaboa, *Acta Biomater.* **2010**, *6*, 1649.
[51] M. Pöttler, A. Fliedner, E. Schreiber, C. Janko, R. P. Friedrich, C. Bohr, M. Döllinger, C. Alexiou, S. Dürr, *Nanoscale Res. Lett.* **2017**, *12*, 284.
[52] M. J. Mokhtari, F. Koohpeima, H. Mohammadi, *Chem. Biol. Drug Des.* **2017**, *90*, 618.
[53] L. F. de A. Vieira, M. P. Lins, I. M. M. N. Viana, J. E. Dos Santos, S. Smaniotto, M. D. D. S. Reis, *Nanoscale Res. Lett.* **2017**, *12*, 200.
[54] Z. Pan, W. Lee, L. Slutsky, R. A. F. Clark, N. Pernodet, M. H. Rafailovich, *Small* **2009**, *5*, 511.
[55] C. M. Kraning-Rush, J. P. Califano, C. A. Reinhart-King, *PLoS One* **2012**, *7*, 32572.
[56] X. L. Wei, Z. H. Mo, B. Li, J. M. Wei, *Colloids Surf., B* **2007**, *59*, 100.
[57] G. Wang, A. H. Dewilde, J. Zhang, A. Pal, M. Vashist, D. Bello, K. A. Marx, S. J. Braunhut, J. M. Therrien, *Part. Fibre Toxicol.* **2011**, *8*, 4.
[58] S. Etienne-Manneville, *Traffic* **2004**, *5*, 470.
[59] J. A. Cooper, *J. Cell Biol.* **1987**, *105*, 1473.
[60] T. Dechat, S. A. Adam, P. Taimen, T. Shimi, R. D. Goldman, *Cold Spring Harbor Perspect. Biol.* **2010**, *2*, 1.
[61] A. Porter, M. Gass, J. Bendall, K. Muller, A. Goode, *ACS Nano* **2009**, *3*, 1485.
[62] B. D. Holt, H. Shams, T. A. Horst, S. Basu, A. D. Rape, Y.-L. Wang, G. K. Rohde, M. R. K. Mofrad, M. F. Islam, K. N. Dahl, *J. Funct. Biomater.* **2012**, *3*, 398.
[63] H. Shams, B. D. Holt, S. H. Mahboobi, Z. Jahed, M. F. Islam, K. N. Dahl, M. R. Mofrad, *ACS Nano* **2013**, *8*, 188.
[64] M. Lundqvist, J. Stigler, T. Cedervall, T. Berggård, M. B. Flanagan, I. Lynch, G. Elia, K. Dawson, *ACS Nano* **2011**, *5*, 7503.
[65] Y. Wen, N. Geitner, R. Chen, F. Ding, *RSC Adv.* **2013**, *3*, 22002.
[66] D. Choudhury, P. L. Xavier, K. Chaudhari, R. John, A. K. Dasgupta, T. Pradeep, G. Chakrabarti, *Nanoscale* **2013**, *5*, 4476.
[67] N. Pernodet, X. Fang, Y. Sun, A. Bakhtina, A. Ramakrishnan, J. Sokolov, A. Ulman, M. Rafailovich, *Small* **2006**, *2*, 766.
[68] R. Pati, I. Das, R. K. Mehta, R. Sahu, A. Sonawane, *Toxicol. Sci.* **2016**, *150*, 454.
[69] L. García-Hevia, R. Valiente, R. Martín-Rodríguez, C. Renero-Lecuna, J. González, L. Rodríguez-Fernández, F. Aguado, J. C. Villegas, M. L. Fanarraga, *Nanoscale* **2016**, *8*, 10963.
[70] A. K. Gupta, M. Gupta, S. J. Yarwood, A. S. G. Curtis, *J. Controlled Release* **2004**, *95*, 197.
[71] V. E. Franklin-Tong, C. W. Gourlay, *Biochem. J.* **2008**, *413*, 389.
[72] L. Gonzalez, M. De Santis Puzzonia, R. Ricci, F. Aureli, G. Guarguaglini, F. Cubadda, L. Leyns, E. Cundari, M. Kirsch-Volders, *Nanotoxicology* **2014**, *5390*, 1.
[73] P. L. Apopa, Y. Qian, R. Shao, N. L. Guo, D. Schwegler-Berry, M. Pacurari, D. Porter, X. Shi, V. Vallyathan, V. Castranova, D. C. Flynn, *Part. Fibre Toxicol.* **2009**, *6*, 1.
[74] A. Mietelska-Porowska, U. Wasik, M. Goras, A. Filipek, G. Niewiadomska, *Int. J. Mol. Sci.* **2014**, *15*, 4671.
[75] G. Hajsalimi, S. Taheri, F. Shahi, L. Pishkar, F. Attar, H. Ahmadi, M. Falahati, *J. Biomol. Struct. Dyn.* **2017**, *1102*, 1.
[76] H. A. Zeinabad, A. Zarrabian, A. A. Saboury, A. M. Alizadeh, M. Falahati, *Sci. Rep.* **2016**, *6*, 26508.
[77] Z. Mao, B. Xu, X. Ji, K. Zhou, X. Zhang, M. Chen, X. Han, Q. Tang, X. Wang, Y. Xia, *Nanoscale* **2015**, *7*, 8466.
[78] F. Xu, C. Piett, S. Farkas, M. Qazzaz, N. I. Syed, *Mol. Brain* **2013**, *6*, 29.
[79] A. Calzado-Martín, M. Encinar, J. Tamayo, M. Calleja, A. San Paulo, *ACS Nano* **2016**, *10*, 3365.
[80] E. L. Elson, *Annu. Rev. Biophys. Biophys. Chem.* **1988**, *17*, 397.
[81] Q. Luo, D. Kuang, B. Zhang, G. Song, *Biochim. Biophys. Acta* **2016**, *1860*, 1953.
[82] J. Pi, F. Yang, H. Jin, X. Huang, R. Liu, P. Yang, J. Cai, *Bioorgan. Med. Chem. Lett.* **2013**, *23*, 6296.
[83] I. V. Ogneva, S. V. Buravkov, A. N. Shubenkov, L. B. Buravkova, *Nanoscale Res. Lett.* **2014**, *9*, 284.
[84] C. C. Zimmer, Y. X. Liu, J. T. Morgan, G. Yang, K.-H. Wang, I. M. Kennedy, A. I. Barakat, G.-Y. Liu, *J. Phys. Chem. B* **2014**, *118*, 1246.
[85] M. R. K. Ali, Y. Wu, D. Ghosh, B. H. Do, K. Chen, M. R. Dawson, N. Fang, T. A. Sulchek, M. A. El-Sayed, *ACS Nano* **2017**, *11*, 3716.
[86] P. Berntsen, C. Y. Park, B. Rothen-Rutishauser, A. Tsuda, T. M. Sager, R. M. Molina, T. C. Donaghey, A. M. Alencar, D. I. Kasahara, T. Ericsson, E. J. Millet, J. Swenson, D. J. Tschumperlin, J. P. Butler, J. D. Brain, J. J. Fredberg, P. Gehr, E. H. Zhou, *J. R. Soc. Interface* **2010**, *7*, S331.
[87] S. Kurosaka, A. Kashina, *Birth Defects Res., Part C* **2008**, *84*, 102.
[88] S. R. Peyton, A. J. Putnam, *J. Cell. Physiol.* **2005**, *204*, 198.
[89] B. S. Verbeek, S. S. Adriaansen-Slot, T. M. Vroom, T. Beckers, G. Rijksen, *FEBS Lett.* **1998**, *425*, 145.
[90] V. Castro Aceituno, S. Ahn, S. Y. Simu, C. Wang, R. Mathiyalagan, D. C. Yang, *In Vitro Cell. Dev. Biol.: Anim.* **2016**, *52*, 1012.
[91] D. Kim, J. Song, S. Kim, H. M. Park, C. H. Chun, J. Sonn, E. J. Jin, *J. Biol. Chem.* **2012**, *287*, 12501.
[92] A. Hall, A. Hall, *Sci. Front. Cell Biol.* **1998**, *279*, 509.
[93] S. Bhattacharya, M. Ahir, P. Patra, S. Mukherjee, S. Ghosh, M. Mazumdar, S. Chattopadhyay, T. Das, D. Chattopadhyay, A. Adhikary, *Biomaterials* **2015**, *51*, 91.
[94] C.-H. Li, P.-L. Liao, M.-K. Shyu, C.-W. Liu, C.-C. Kao, S.-H. Huang, Y.-W. Cheng, J.-J. Kang, *Toxicol. Sci.* **2012**, *126*, 162.
[95] S. Krugmann, I. Jordens, K. Gevaert, M. Driessens, J. Vandekerckhove, A. Hall, *Curr. Biol.* **2001**, *11*, 1645.
[96] T. Zhou, M. Yu, B. Zhang, L. Wang, X. Wu, H. Zhou, Y. Du, J. Hao, Y. Tu, C. Chen, T. Wei, *Adv. Funct. Mater.* **2014**, *24*, 6922.
[97] Y. F. Xiao, J. M. Li, S. M. Wang, X. Yong, B. Tang, M. M. Jie, H. Dong, X. C. Yang, S. M. Yang, *Int. J. Nanomed.* **2016**, *11*, 3023.

[98] K. Mosallanejad, Y. Sekine, S. Ishikura-Kinoshita, K. Kumagai, T. Nagano, A. Matsuzawa, K. Takeda, I. Naguro, H. Ichijo, *Sci. Signal.* **2014**, *7*, 40.

[99] B. Hong, H. Li, M. Zhang, J. Xu, Y. Lu, Y. Zheng, J. Qian, J. T. Chang, J. Yang, Q. Yi, *Int. J. Cancer* **2015**, *136*, 34.

[100] R. R. Arvizo, S. Saha, E. Wang, J. D. Robertson, R. Bhattacharya, *Proc. Natl. Acad. Sci. USA* **2013**, *110*, 6700.

[101] M. Miettinen, M.-S. Rikala, J. Rysz, J. Lasota, Z.-F. Wang, *Am. J. Surg. Pathol.* **2012**, *36*, 629.

[102] Y. Pan, Q. Wu, L. Qin, J. Cai, B. Du, *Biomed Res. Int.* **2014**, *2014*, 1.

[103] Z. Liu, Y. Wu, Z. Guo, Y. Liu, Y. Shen, P. Zhou, X. Lu, *PLoS One* **2014**, *9*, 1.

[104] L. Huang, B. Xia, Z. Liu, Q. Cao, J. Huang, Z. Luo, *Front. Cell. Neurosci.* **2017**, *11*, 1.

[105] S. Sharifi, S. Behzadi, S. Laurent, M. L. Forrest, P. Stroeve, M. Mahmoudi, *Chem. Soc. Rev.* **2012**, *41*, 2323.

[106] M. C. Stensberg, Q. Wei, E. S. McLamore, D. M. Porterfield, A. Wei, M. S. Sepulveda, *Nanomedicine* **2011**, *6*, 879.

[107] E. S. Glazer, C. Zhu, A. N. Hamir, A. Borne, C. S. Thompson, S. A. Curley, *Nanotoxicology* **2011**, *5*, 459.

[108] T. Xia, M. Kovochich, M. Liong, L. Madler, B. Gilbert, H. Shi, J. I. Yeh, J. I. Zink, A. E. Nel, *ACS Nano* **2008**, *2*, 2121.

[109] B. Yue, *J. Glaucoma* **2014**, *23*, 20.

[110] M. J. Dalby, N. Gadegaard, R. O. C. Oreffo, *Nat. Mater.* **2014**, *13*, 558.

[111] M. Miyaki, K. Fujimoto, H. Kawaguchi, *Colloids Surf., A* **1999**, *153*, 603.

[112] B. G. Cousins, P. J. Doherty, R. L. Williams, J. Fink, M. J. Garvey, *J. Mater. Sci. Mater. Med.* **2004**, *15*, 355.

[113] B. G. Cousins, H. E. Allison, P. J. Doherty, C. Edwards, M. J. Garvey, D. S. Martin, R. L. Williams, *J. Appl. Microbiol.* **2007**, *102*, 757.

[114] M. Arnold, M. Schwieder, J. Blummel, E. A. Cavalcanti-Adam, M. Lopez-Garcia, H. Kessler, B. Geiger, J. P. Spatz, *Soft Matter* **2009**, *5*, 72.

[115] H. Lee, Y. Jang, J. Seo, J. M. Nam, K. Char, *ACS Nano* **2011**, *5*, 5444.

[116] J. Albuschies, V. Vogel, *Sci. Rep.* **2013**, *1658*, 1.

[117] F. C. Schenk, H. Boehm, J. P. Spatz, S. V. Wegner, *Langmuir* **2014**, *30*, 6897.

[118] P. Li, K. Greben, R. Wördenweber, U. Simon, A. Offenhäusser, D. Mayer, *RSC Adv.* **2015**, *5*, 39252.

[119] F. L. Yap, Y. Zhang, *Biomaterials* **2007**, *28*, 2328.

[120] M. Arnold, V. C. Hirschfeld-Warneken, T. Lohmüller, P. Heil, J. Blümmel, E. A. Cavalcanti-Adam, M. López-García, P. Walther, H. Kessler, B. Geiger, J. P. Spatz, *Nano Lett.* **2008**, *8*, 2063.

[121] R. Palankar, N. Medvedev, A. Rong, M. Delcea, *ACS Nano* **2013**, *7*, 4617.

[122] W. Luo, M. N. Yousaf, *Chem. Commun.* **2009**, 1237.

[123] Z. Lyu, H. Wang, Y. Wang, K. Ding, H. Liu, L. Yuan, X. Shi, M. Wang, Y. Wang, H. Chen, *Nanoscale* **2014**, *6*, 6959.

[124] J.-H. Lee, W. Shim, N. Choolakadavil Khalid, W.-S. Kang, M. Lee, H.-S. Kim, J. Choi, G. Lee, J.-H. Kim, *ACS Appl. Mater. Interfaces* **2015**, *7*, 1560.

[125] N. S. Kehr, S. Atay, B. Ergün, *Macromol. Biosci.* **2015**, *15*, 445.

[126] I. Platzman, C. A. Muth, C. Lee-Thedieck, D. Pallarola, R. Atanasova, I. Louban, E. Altrock, J. P. Spatz, *RSC Adv.* **2013**, *3*, 13293.

[127] T. Velnar, T. Bailey, V. Smrkolj, *J. Int. Med. Res.* **2009**, *37*, 1528.

[128] S. Huang, D. E. Ingber, *Cancer Cell* **2005**, *8*, 175.

[129] J. Kim, J. Yoon, R. C. Hayward, *Nat. Mater.* **2010**, *9*, 159.

[130] K. A. Davis, K. A. Burke, P. T. Mather, J. H. Henderson, *Biomaterials* **2011**, *32*, 2285.

[131] K. Uto, M. Ebara, T. Aoyagi, *Int. J. Mol. Sci.* **2014**, *15*, 1511.

[132] M. T. Frey, Y. Wang, *Soft Matter* **2009**, *5*, 1918.

[133] H. Y. Yoshikawa, F. F. Rossetti, S. Kaufmann, T. Kaindl, J. Madsen, U. Engel, A. L. Lewis, S. P. Armes, M. Tanaka, *J. Am. Chem. Soc.* **2011**, *133*, 1367.

[134] J. D. Kiang, J. H. Wen, J. C. Del Álamo, A. J. Engler, *J. Biomed. Mater. Res., Part A* **2013**, *101 A*, 2313.

[135] Y. Li, G. Huang, X. Zhang, B. Li, Y. Chen, T. Lu, T. J. Lu, F. Xu, *Adv. Funct. Mater.* **2013**, *23*, 660.

[136] M. Mayer, R. Rabindranath, J. Börner, E. Hörner, A. Bentz, J. Salgado, H. Han, H. Böse, J. Probst, M. Shamonin, G. J. Monkman, G. Schlunck, *PLoS One* **2013**, *8*, 1.

[137] T. Iskratsch, H. Wolfenson, M. P. Sheetz, *Nat. Rev. Mol. Cell Biol.* **2014**, *15*, 825.

[138] S. V Plotnikov, A. M. Pasapera, B. Sabass, C. M. Waterman, *Cell* **2012**, *151*, 1513.

[139] A. K. Harris, P. Wild, D. Stopak, *Science* **1980**, *208*, 177.

[140] M. Gupta, L. Kocgozlu, B. R. Sarangi, F. Margadant, M. Ashraf, B. Ladoux, *Methods Cell Biol.* **2015**, *125*, 289.

[141] M. Dembo, Y.-L. Wang, *Biophys. J.* **1999**, *76*, 2307.

[142] M. L. Lombardi, D. A. Knecht, M. Dembo, J. Lee, *J. Cell Sci.* **2007**, *120*, 1624.

[143] H. Delanoe-Ayari, J. P. Rieu, M. Sano, *Phys. Rev. Lett.* **2010**, *105*, 2.

[144] C. Franck, S. A. Maskarinec, D. A. Tirrell, G. Ravichandran, *PLoS One* **2011**, *6*, 1.

[145] J. P. Butler, I. M. Tolic-Norrelykke, B. Fabry, J. J. Fredberg, *Am. J. Physiol. Cell Physiol.* **2002**, *282*, 595.

[146] J. Notbohm, J. H. Kim, C. Franck, S. Maskarinec, D. Tirrell, A. Asthagiri, G. Ravichandran, *Proc. IUTAM* **2012**, *4*, 144.

[147] J. H. Wang, J. Lin, *Biomech. Model. Mechanobiol.* **2007**, *6*, 361.

[148] R. W. Style, R. Boltyanskiy, G. K. German, C. Hyland, C. W. Macminn, A. F. Mertz, L. A. Wilen, Y. Xu, E. R. Dufresne, *Soft Matter* **2014**, *10*, 4047.

[149] U. S. Schwarz, J. R. D. Soiné, *Biochim. Biophys. Acta* **2015**, *1853*, 3095.

[150] W. R. Legant, C. K. Choi, J. S. Miller, L. Shao, L. Gao, E. Betzig, C. S. Chen, *Proc. Natl. Acad. Sci. USA* **2013**, *110*, 881.

[151] B. Álvarez-González, S. Zhang, M. Gómez-González, R. Meili, R. A. Firtel, J. C. Lasheras, J. C. Del Alamo, *Sci. Rep.* **2017**, *7*, 39315.

[152] H. Colin-York, D. Shrestha, J. H. Felce, D. Waithe, E. Moeendarbary, S. J. Davis, C. Eggeling, M. Fritzsche, *Nano Lett.* **2016**, *16*, 2633.

[153] M. Bergert, T. Lendenmann, M. Zundel, A. E. Ehret, D. Panozzo, P. Richner, D. K. Kim, S. J. P. Kress, D. J. Norris, O. Sorkine-hornung, E. Mazza, D. Poulikakos, A. Ferrari, *Nat. Commun.* **2016**, *7*, 12814.

[154] C. N. Holenstein, U. Silvan, J. G. Snedeker, *Sci. Rep.* **2017**, *7*, 41633.

[155] Y. Han, J. Wang, K. Wang, S. Dong, *Micro Nano Lett.* **2016**, *11*, 881.

[156] H. Babahosseini, B. Carmichael, J. S. Strobl, S. N. Mahmoodi, M. Agah, *Biochem. Biophys. Res. Commun.* **2015**, *463*, 587.

[157] D. J. Müller, Y. F. Dufrêne, *Trends Cell Biol.* **2011**, *21*, 461.

[158] S. Iyer, R. Gaikwad, V. Subba-Rao, C. D. Woodworth, I. Sokolov, *Nat. Nanotechnol.* **2011**, *4*, 389.

[159] D. Kirmizis, S. Logothetidis, *Int. J. Nanome* **2010**, *5*, 137.

[160] T. Bongiorno, J. L. Chojnowski, J. D. Lauderdale, T. Sulchek, *Biophys. J.* **2016**, *111*, 1761.

[161] S. Nawaz, P. Sanchez, K. Bodensiek, S. Li, M. Simons, I. A. T. Schaap, *PLoS One* **2012**, *7*, 1.

[162] M. Nikkhah, J. S. Strobl, E. M. Schmelz, M. Agah, *J. Biomech.* **2011**, *44*, 762.

[163] H. Schillers, M. Wälte, K. Urbanova, H. Oberleithner, *Biophys. J.* **2010**, *99*, 3639.

[164] Y. A. Ayala, B. Pontes, D. S. Ether, L. B. Pires, G. R. Araujo, S. Frases, L. F. Romão, M. Farina, V. Moura-Neto, N. B. Viana, H. M. Nussenzveig, *BMC Biophys.* **2016**, *9*, 5.

[165] Y. A. Ayala, B. Pontes, B. Hissa, A. C. M. Monteiro, M. Farina, V. Moura-Neto, N. B. Viana, H. M. Nussenzveig, *Exp. Cell Res.* **2017**, *351*, 173.
[166] M. Schwingel, M. Bastmeyer, *PLoS One* **2013**, *8*, 1.
[167] K. Mandal, A. Asnacios, B. Goud, J.-B. Manneville, *Proc. Natl. Acad. Sci. USA* **2016**, *113*, E7159.
[168] F. Etoc, D. Lisse, Y. Bellaiche, J. Piehler, M. Coppey, M. Dahan, *Nat. Nanotechnol.* **2013**, *8*, 193.
[169] M. B. Steketee, S. N. Moysidis, X.-L. Jin, J. E. Weinstein, W. Pita-Thomas, H. B. Raju, S. Iqbal, J. L. Goldberg, *Proc. Natl. Acad. Sci. USA* **2011**, *108*, 19042.
[170] P. Tseng, J. W. Judy, D. Di Carlo, *Nat. Methods* **2012**, *9*, 1113.
[171] J.-F. Berret, *Nat. Commun.* **2016**, *7*, 9.
[172] R. J. Marjoram, C. Guilluy, K. Burridge, *Methods* **2016**, *94*, 19.
[173] Y.-Q. Chen, C.-Y. Kuo, M.-T. Wei, K. Wu, P.-T. Su, C.-S. Huang, A. Chiou, *J. Biomed. Opt.* **2013**, *19*, 11008.
[174] D. Ghosh, L. Lili, D. J. McGrail, L. V Matyunina, J. F. McDonald, M. R. Dawson, *Stem Cells Dev.* **2014**, *23*, 245.
[175] Y.-Q. Chen, Y.-S. Liu, Y.-A. Liu, Y.-C. Wu, J. C. Del Álamo, A. Chiou, O. K. Lee, *Sci. Rep.* **2016**, *6*, 31547.
[176] V. Panzetta, I. Musella, I. Rapa, M. Volante, P. A. Netti, S. Fusco, *Acta Biomater.* **2017**, *57*, 334.
[177] G. Binnig, C. Quate, C. Gerber, *Phys. Rev. Lett.* **1986**, *56*, 930.
[178] G. Haugstad, *Atomic Force Microscopy*, John Wiley & Sons, Inc., Hoboken, NJ, USA **2012**.
[179] H. J. Butt, B. Cappella, M. Kappl, *Surf. Sci. Rep.* **2005**, *59*, 1.
[180] A. B. Drake, C. B. Prater, A. L. Weisenhorn, S. A. C. Gould, T. R. Albrecht, D. S. Cannell, H. G. Hansma, P. K. Hansma, *Science* **1989**, *243*, 1586.
[181] C. S. Hodges, *Adv. Colloid Interface Sci.* **2002**, *99*, 13.
[182] D. Ricci, M. Tedesco, M. Grattarola, *Microsc. Res. Tech.* **1997**, *36*, 165.
[183] G. T. Charras, M. A. Horton, *Biophys. J.* **2002**, *83*, 858.
[184] A. Cartagena, A. Raman, *Biophys. J.* **2014**, *106*, 1033.
[185] T. G. Kuznetsova, M. N. Starodubtseva, N. I. Yegorenkov, S. A. Chizhik, R. I. Zhdanov, *Micron* **2007**, *38*, 824.
[186] H. Liu, J. Wen, Y. Xiao, J. Liu, S. Hopyan, M. Radisic, C. A. Simmons, Y. Sun, *ACS Nano* **2014**, *8*, 3821.
[187] M. Li, L. Liu, X. Xiao, N. Xi, Y. Wang, *IEEE Trans. Nanobioscience* **2016**, *15*, 398.
[188] S. Hiratsuka, Y. Mizutani, A. Toda, N. Fukushima, K. Kawahara, H. Tokumoto, T. Okajima, *Jpn. J. Appl. Phys.* **2009**, *48*, 1.
[189] T. Okajima, M. Tanaka, S. Tsukiyama, T. Kadowaki, S. Yamamoto, M. Shimomura, H. Tokumoto, *Jpn. J. Appl. Phys.* **2007**, *46*, 5552.
[190] B. Fallqvist, M. L. Fielden, T. Pettersson, N. Nordgren, M. Kroon, A. K. B. Gad, *J. Mech. Behav. Biomed. Mater.* **2016**, *59*, 168.
[191] N. R. Wilson, J. V. Macpherson, *Nat. Nanotechnol.* **2009**, *4*, 483.
[192] N. A. Kouklin, W. E. Kim, A. D. Lazareck, J. M. Xu, *Appl. Phys. Lett.* **2005**, *87*, 1.
[193] I. U. Vakarelski, S. C. Brown, K. Higashitani, B. M. Moudgil, *Langmuir* **2007**, *23*, 10893.
[194] J. E. Koehne, R. M. Stevens, T. Zink, Z. Deng, H. Chen, I. C. Weng, F. T. Liu, G. Y. Liu, *Ultramicroscopy* **2011**, *111*, 1155.
[195] X. Chen, A. Kis, A. Zettl, C. R. Bertozzi, *Proc. Natl. Acad. Sci. USA* **2007**, *104*, 8218.
[196] I. Obataya, C. Nakamura, S. Han, N. Nakamura, J. Miyake, *Nano Lett.* **2005**, *5*, 27.
[197] A. TermehYousefi, S. Bagheri, S. Shahnazar, M. H. Rahman, N. A. Kadri, *Mater. Sci. Eng. C* **2016**, *59*, 636.
[198] A. Ashkin, J. M. Dziedzic, J. E. Bjorkholm, S. Chu, *Opt. Lett.* **1986**, *11*, 288.
[199] F. M. Hochmuth, J. Y. Shao, J. Dai, M. P. Sheetz, *Biophys. J.* **1996**, *70*, 358.
[200] D. Raucher, M. P. Sheetz, *Biophys. J.* **1999**, *77*, 1992.
[201] W. W. Ahmed, É. Fodor, T. Betz, *Biochim. Biophys. Acta, Mol. Cell Res.* **2015**, *1853*, 3083.
[202] B. Pontes, Y. Ayala, A. C. C. Fonseca, L. F. Romào, R. F. Amal, L. T. Salgado, F. R. Lima, M. Farina, N. B. Viana, V. Moura-Neto, H. M. Nussenveig, *PlosOne* **2013**, *8*, 1.
[203] M. Allioux-Guérin, D. Icard-Arcizet, C. Durieux, S. Hénon, F. Gallet, J.-C. Mevel, M.-J. Masse, M. Tramier, M. Coppey-Moisan, *Biophys. J.* **2009**, *96*, 238.
[204] D. Raucher, T. Stauffer, W. Chen, K. Shen, S. Guo, J. D. York, M. P. Sheetz, T. Meyer, *Cell* **2000**, *100*, 221.
[205] I. Titushkin, M. Cho, *Biophys. J.* **2006**, *90*, 2582.
[206] S. Khatibzadeh, Nima, Gupta , *Soft Matter* **2012**, *8*, 8350.
[207] M. Capitanio, F. S. Pavone, *Biophys. J.* **2013**, *105*, 1293.
[208] M. Castillo, R. Ebensperger, D. Wirtz, M. Walczak, D. E. Hurtado, A. Celedon, *J. Biomed. Mater. Res., Part B* **2015**, *102*, 1779.
[209] A. Celedon, C. M. Hale, D. Wirtz, *Biophys. J.* **2011**, *101*, 1880.
[210] N. Wang, J. P. P. Butler, D. E. E. Ingber, *Science* **1993**, *260*, 1124.
[211] M. Glogauer, P. Arora, G. Yao, I. Sokholov, J. Ferrier, C. A. McCulloch, *J. Cell Sci.* **1997**, *21*, 11.
[212] M. Glogauer, J. Ferrier, C. A. McCulloch, *Am. J. Physiol.* **1995**, *269*, 1093.
[213] C. Guilluy, L. D. Osborne, L. L. Van, L. Sharek, R. Superfine, R. Garcia-Mata, K. Burridge, *Nat. Cell Biol.* **2014**, *16*, 376.
[214] B. D. Matthews, D. R. Overby, R. Mannix, D. E. Ingber, *J. Cell Sci.* **2006**, *119*, 508.
[215] X. Trepat, L. Deng, S. S. An, D. Navajas, D. J. Tschumperlin, W. T. Gerthoffer, J. P. Butler, J. J. Fredberg, *Nature* **2007**, *447*, 592.
[216] N. J. Sniadecki, *Endocrinology* **2010**, *151*, 451.
[217] X. Trepat, G. Lenormand, J. J. Fredberg, *Soft Matter* **2008**, *4*, 1750.
[218] M. Versaevel, M. Riaz, T. Corne, T. Grevesse, J. Lantoine, D. Mohammed, C. Bruyére, L. Alaimo, W. H. De Vos, S. Gabriele, *Cell Adhes. Migr.* **2017**, *11*, 98.
[219] C. Schmidt, H. Pommerenke, F. Dürr, B. Nebe, J. Rychly, *J. Biol. Chem.* **1998**, *273*, 5081.
[220] F. J. Alenghat, B. Fabry, K. Y. Tsai, W. H. Goldmann, D. E. Ingber, *Biochem. Biophys. Res. Commun.* **2000**, *277*, 93.
[221] J. C. Berrios, M. A. Schroeder, R. D. Hubmayr, J. C. Berrios, M. A. Schroeder, R. D. Hubmayr, *J. Appl. Physiol.* **2001**, *91*, 65.
[222] J. Chen, B. Fabry, E. L. Schiffrin, N. Wang, *Am. J. Physiol. Cell Physiol.* **2001**, *280*, 1475.
[223] Z. Wu, K. Wong, M. Glogauer, R. P. Ellen, C. a McCulloch, *Biochem. Biophys. Res. Commun.* **1999**, *261*, 419.
[224] L. Balasubramanian, A. Ahmed, C.-M. Lo, J. S. K. Sham, K.-P. Yip, *Am. J. Physiol.: Regul., Integr. Comp. Physiol.* **2007**, *293*, 1586.
[225] U. S. Potard, J. P. Butler, N. Wang, *Am. J. Physiol.* **1997**, *272*, 1654.
[226] M. Yoshida, W. F. Westlin, N. Wang, D. E. Ingber, A. Rosenzweig, N. Resnick, M. A. Gimbrone, *J. Cell Biol.* **1996**, *133*, 445.
[227] M. Machacek, L. Hodgson, C. Welch, H. Elliott, P. Nalbant, A. Abell, G. L. Johnson, K. M. Hahn, G. Danuser, *Nature* **2009**, *461*, 99.
[228] R. Zhao, T. Boudou, W. G. Wang, C. S. Chen, D. H. Reich, *Adv. Mater.* **2013**, *25*, 1699.
[229] R. Zhao, T. Boudou, W. G. Wang, C. S. Chen, D. H. Reich, *J. Appl. Phys.* **2014**, *115*, 1.
[230] F. Xu, R. Zhao, A. S. Liu, T. Metz, Y. Shi, P. Bose, *Lab Chip* **2015**, *15*, 2496.
[231] Y. Tseng, T. P. Kole, D. Wirtz, *Biophys. J.* **2002**, *83*, 3162.
[232] D. Wirtz, *Annu. Rev. Biophys.* **2009**, *38*, 301.
[233] K. M. Schultz, K. a Kyburz, K. S. Anseth, *Proc. Natl. Acad. Sci. USA* **2015**, *112*, 3757.
[234] M. Mak, R. D. Kamm, M. H. Zaman, *PLoS Comput. Biol.* **2014**, *10*, 1.

[235] A. M. Smelser, J. C. Macosko, A. P. O'Dell, S. Smyre, K. Bonin, G. Holzwarth, *Biomech. Model. Mechanobiol.* **2015**, *14*, 1335.
[236] P.-H. Wu, C. M. Hale, W.-C. Chen, J. S. H. Lee, Y. Tseng, D. Wirtz, *Nat. Protoc.* **2012**, *7*, 155.
[237] J. S. H. Lee, P. Panorchan, C. M. Hale, S. B. Khatau, T. P. Kole, Y. Tseng, D. Wirtz, *J. Cell Sci.* **2006**, *119*, 1760.
[238] J. H. Dangaria, P. J. Butler, *Am. J. Physiol. Cell Physiol.* **2007**, *293*, 1568.
[239] C. Picard, A. Donald, *Eur. Phys. J. E* **2009**, *30*, 127.
[240] E. L. Baker, R. T. Bonnecaze, M. H. Zaman, *Biophys. J.* **2009**, *97*, 1013.
[241] V. Panzetta, M. De Menna, I. Musella, M. Pugliese, M. Quarto, P. A. Netti, S. Fusco, *Cytoskeleton* **2017**, *74*, 40.
[242] K. M. McAndrews, D. J. McGrail, N. D. Quach, M. R. Dawson, *Phys. Biol.* **2012**, *76*, 211.